Received: 21 August 2018 | Revised: 27 February 2019 | Accepted: 2 March 2019

DOI: 10.1002/dvdy.23

PATTERNS & PHENOTYPES

Developmental Dynamics WILEY

LPA_1, LPA_2, LPA_4, and LPA_6 receptor expression during mouse brain development

Olga Suckau[1] | Isabel Gross[2,3] | Sandra Schrötter[1] | Fan Yang[4] | Jiankai Luo[4] | Andreas Wree[2] | Jerold Chun[5] | David Baska[6] | Jan Baumgart[6] | Kuniyuki Kano[7] | Junken Aoki[7] | Anja U. Bräuer[1,2,3,8]

[1]Institute of Cell Biology and Neurobiology, Center for Anatomy, Charité–Universitätsmedizin Berlin, Berlin, Germany

[2]Institute of Anatomy, Universitätsmedizin Rostock, Rostock, Germany

[3]Research Group Anatomy, School of Medicine and Health Sciences, Carl von Ossietzky University Oldenburg, Oldenburg, Germany

[4]Albrecht Kossel Institute for Neuroregeneration, Rostock University Medical Center, Rostock, Germany

[5]Department of Molecular and Cellular Neuroscience, The Scripps Research Institute, La Jolla, California

[6]Translational Animal Research Center, University Medical Center of the Johannes Gutenberg–University Mainz, Mainz, Germany

[7]Graduate School of Pharmaceutical Science, University of Tokyo, Tokyo, Japan

[8]Research Center for Neurosensory Science, Carl von Ossietzky University Oldenburg, Oldenburg, Germany

Correspondence
Anja U. Bräuer, School of Medicine and Health Sciences, Carl von Ossietzky University Oldenburg, Department of Human Medicine, Division of Anatomy, Carl von Ossietzky Str. 9-11, 26129 Oldenburg, Germany.
Email: anja.braeuer@uni-oldenburg.de

Funding information
This work was supported by the DFG BR 2345/1-1 and the IBB to A.U.B., and by the Sonnenfeld-Stiftung for sponsoring technical equipment for A.U.B.

Abstract

Background: LPA is a small bioactive phospholipid that acts as an extracellular signaling molecule and is involved in cellular processes, including cell proliferation, migration, and differentiation. LPA acts by binding and activating at least six known G protein–coupled receptors: $LPA_{1–6}$. In recent years, LPA has been suggested to play an important role both in normal neuronal development and under pathological conditions in the nervous system.

Results: We show the expression pattern of LPA receptors during mouse brain development by using qRT-PCR, in situ hybridization, and immunocytochemistry. Only *LPA_1*, *LPA_2*, *LPA_4*, and *LPA_6* mRNA transcripts were detected throughout development stages from embryonic day 16 until postnatal day 30 of hippocampus, neocortex, cerebellum, and bulbus olfactorius in our experiments, while expression of *LPA_3* and *LPA_5* genes was below detection level. In addition to our qRT-PCR results, we also analyzed the cellular protein expression of endogenous LPA receptors, with focus on LPA_1 and LPA_2 within postnatal brain slices and primary neuron differentiation with and without cytoskeleton stabilization and destabilization.

Conclusions: The expression of LPA receptors changes depends on the developmental stage in mouse brain and in cultured hippocampal primary neurons. Interestingly, we found that commercially available antibodies for LPA receptors are largely unspecific.

Olga Suckau and Isabel Gross contributed equally to this work.

KEYWORDS
G protein–coupling receptor, growth cone, lysophosphatidic acid, microtubule, primary brain cells, qRT-PCR

1 | INTRODUCTION

Lysophosphatidic acid (LPA) is a bioactive phospholipid present in biological fluids and tissue, including brain.[1–4] LPA induces a wide range of cellular responses on primary brain cells and neural progenitors, including intracellular calcium mobilization,[5–7] growth cone collapse and neurite retraction,[1,8–10] cell survival and apoptosis,[11–13] cell proliferation and differentiation,[5,12,14–16] altered postmitotic neuronal migration,[17] and myelination in the central nervous system (CNS).[16,18–21]

LPA-induced effects are mediated through binding to and activation of a specific class of G protein–coupled receptors (GPCRs). To date, six cell-surface receptors have been identified: LPA_1 (EDG2), LPA_2 (EDG4), LPA_3 (EDG7), LPA_4 (GPR23/P2Y9), LPA_5 (GPR92), and LPA_6 (P2Y5).[3,22–29] Activated LPA receptors couple with several types of G proteins to trigger a wide range of different downstream signaling pathways: for example, activation of phospholipase C, Rho, Akt, and phosphatidylinositol 3–kinase pathways, or inhibition of adenylyl cyclase.[26,30–33] This in turn mediates the cellular responses as described above. The LPA-induced effects may result from differences in concentration and differential expression of various LPA receptor subtypes. The LPA receptor gene products are detectable in most mammalian tissues in spatial and temporal expression patterns, but a systematic analysis in the developing brain of all six LPA receptors is not yet available.

However, extracellular LPA levels or other phospholipids are known to increase in response to brain injury.[5,34–36] Furthermore, changes in LPA concentration and LPA receptor or LPA metabolic enzyme expression have been linked to neurological disorders such as schizophrenia,[37,38] cancer growth, metastasis,[32,39,40] and neuropathic pain.[41,42] These observations underline the importance of LPA signaling both in normal development and under pathological conditions in the nervous system and suggest that LPA receptors could be drug targets for therapeutic intervention.

Although a large number of publications on LPA receptor gene expression is available, only one study, results of which were published by Ohuchi et al,[43] has begun systematic analysis of $LPA_{1–5}$ transcript distribution during mouse organogenesis. Previous publication partly shows discrepancy of *LPA* receptor gene expression, which may be the result of different detection methods. Unfortunately, LPA receptor expression at protein level is unknown due to the lack of specific antibodies.[44]

Our study examined the expression pattern of $LPA_{1–6}$ receptor transcripts in different mouse brain areas by using different molecular biological techniques to determine gene regulation from late embryonic developmental stages to adulthood. In this phase of life, neurogenesis is almost completed, and astrogenesis and oligodendrogenesis start. During the first postnatal weeks, axons and dendrites continue to grow and mature, followed by synapse formation, maturation, and stabilization.[45,46] It has been shown that in all these processes, LPA plays an important role, such as in timing of outgrowth, cell migration, myelination, cell survival, and modulating synaptic function.[47]

Furthermore, we aimed to identify specific LPA receptor antibodies using multiple specificity tests. Therefore, for the first time we were able to show the protein expression dynamics of LPA receptors on cellular and subcellular levels.

2 | RESULTS

2.1 | LPA_1, LPA_2, LPA_4, and LPA_6 receptors predominate and are dynamically expressed during mouse brain development

The group of Dr Noji[43] reported on the gene expression pattern of $LPA_{1–5}$ receptors in whole mouse embryos from embryonic day 8.5 (E8.5) to E12.5, which they determined using whole-mount in situ hybridization (ISH) technique. We used their research as the basis for our study, extending the analysis to the time period from E16 to postnatal day 30 (P30), when astrogenesis, oligodendrogenesis, axon and dendrite outgrowth, and synapse formation take place. We also included the novel LPA receptor LPA_6 in our analysis. Gene expression of the six *LPA* receptors was analyzed in hippocampus, neocortex, cerebellum, and bulbus olfactorius using quantitative real-time PCR (qRT-PCR) (Figure 1). Overall, while dynamically expressed, LPA_1, LPA_2, LPA_4, and LPA_6 (Figure 1A–D) were detected throughout all developmental stages and in all brain regions tested, as described in more detail below; LPA_3 and LPA_5 expression remained below detection level (Figure 1A–D).

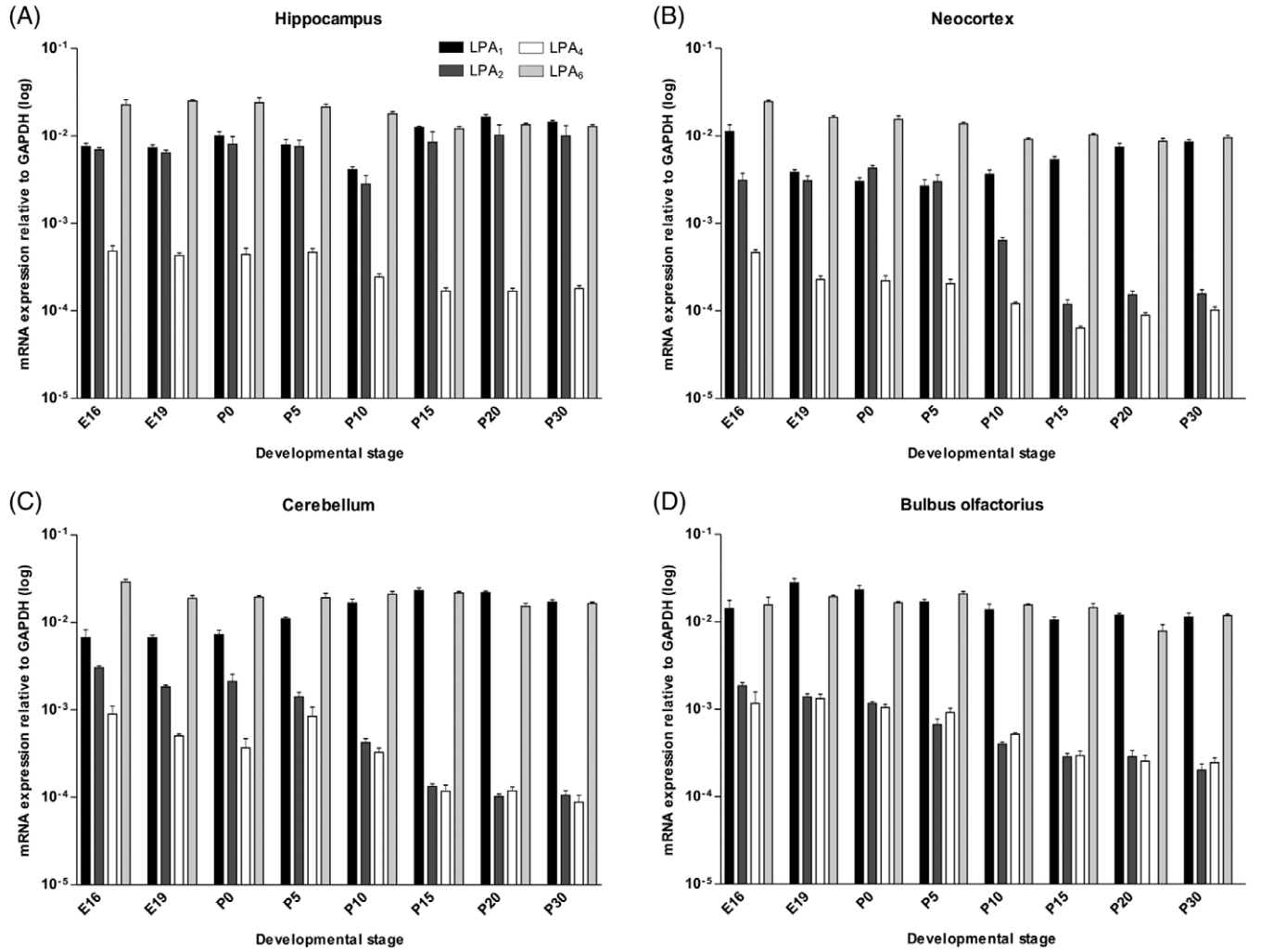

FIGURE 1 Gene expression profile of *LPA* receptors during mouse brain development. Analysis of $LPA_{1\text{-}6}$ receptor gene expression in hippocampus (A), neocortex (B), cerebellum (C), and bulbus olfactorius (D) between E16 and P30. The expression levels of each receptor transcript for each sample were normalized to GAPDH. E, embryonic day; P, postnatal day. Error bars represent SD (n = 3)

2.1.1 | Hippocampus

The hippocampal region exhibited dynamic expression of LPA_1, LPA_2, LPA_4, and LPA_6 receptor transcripts (Figure 1A). Throughout all analyzed developmental stages, LPA_1, LPA_2, and LPA_6 expression was at least 10-fold higher than LPA_4 receptor transcripts (Figure 1A). Only in the hippocampus were LPA_1, LPA_2, and LPA_6 receptors almost constitutively expressed during development.

2.1.2 | Neocortex

The LPA_1 receptor was present at almost the same level in neocortical tissue as in the hippocampus throughout the investigated developmental stages (Figure 1B). Over time, a slight U-type course with a minimum gene expression around birth could be detected (Figure 1B). LPA_2 transcripts showed no changes in expression at embryonic stages up to P5. After P5, the LPA_2 receptor showed a strong down-regulation (up to 10-fold) until P15 and then remained stable at this low level until P30 (Figure 1B). The LPA_4 receptor decreased slightly from E16, reaching its minimum at P15. At P20 and P30, the expression of LPA_4 receptor rose again slightly (Figure 1B). The LPA_6 receptor was almost constitutively expressed, as found in the hippocampus (Figure 1B).

2.1.3 | Cerebellum

In cerebellum, the LPA_1 transcript level showed weak up-regulation after birth and peaked at P15 (Figure 1C). In contrast, LPA_2 and LPA_4 transcripts decreased consistently over time, with the exception of P5, where LPA_4 showed an up-regulation to the level of E16. At E16 and E19, the expression of LPA_2 transcripts was 5-fold weaker compared to that of

LPA4. After birth the two receptors showed equal expression pattern, and from P15 the transcripts remained stable (Figure 1C). The *LPA6* receptor was almost constitutively expressed, similar to hippocampus and neocortex (Figure 1C).

2.1.4 | Bulbus olfactorius

LPA1 mRNA expression was high in bulbus olfactorius and increased slightly at stages E19 and P0 (Figure 1D). The expression was at least 10-fold higher (at E16) than that of *LPA2* or *LPA4* receptors throughout all analyzed developmental stages, with the greatest difference in values at P30. The gene levels of *LPA2* and *LPA4* receptors were similar and were consistently down-regulated between E16 and P30 (Figure 1D). Of all brain areas analyzed, bulbus olfactorius exhibited the lowest expression of *LPA2* and *LPA4* throughout all investigated development stages (Figure 1D). Again, the *LPA6* receptor mRNA was almost constitutively expressed in the same expression level as *LPA1* (Figure 1D).

2.2 | Cellular localization of *LPA1*, *LPA2*, *LPA4*, and *LPA6* receptor mRNA in postnatal stages of different mouse brain areas

For verification of qRT-PCR results and cellular localization, we performed ISH of *LPA1, LPA2, LPA4,* and *LPA6* receptors in hippocampus/dentate gyrus, neocortex, cerebellum, and bulbus olfactorius in P0, P10, and P30 (Figure 2) developmental stages.

LPA1 mRNA was detected in all examined brain areas and all developmental stages in high amounts, with very strong signals in white matter regions such as the corpus callosum and arbor vitae of the cerebellum, where oligodendrocytes predominantly are located, as well as in compact neuronal structures like the dentate gyrus of the hippocampus (Figure 2A). Also, in non-neuronal cells, the *LPA1* mRNA expression was detectable, like in leptomeninges, covering the neocortex.

A decrease in *LPA2* mRNA during development could be observed in all examined regions, as well as in the hippocampus, where qRT-PCR did not show developmental mRNA decrease (Figure 2B). However, the *LPA2* mRNA signal in particular is detectable in compact neuronal structures.

As indicated by qRT-PCR, *LPA4* signal was detected only weakly throughout the brain, with a slight decrease in more mature stages, but still detectable in compact neuronal structures, like the dentate gyrus (Figure 2C).

LPA6 receptor mRNA showed weaker signal then expected from qRT-PCR results but was clearly detectable throughout all examined areas and stages. ISH confirmed its continuous and overall expression during mouse brain development and showed signals in compact neuronal regions, as well as in brain regions where non-neuronal cells are mainly located, such as white matter of the arbor vitae of the cerebellum or leptomeninges (Figure 2D).

2.3 | LPA_1 and LPA_2 receptor protein expression and N-glycosylation in mouse brain

Many commercially available antibodies against synthetic peptides corresponding to regions of human or mouse LPA receptor proteins have never been analyzed for their specificity.[48,49] We have comprehensively evaluated seven commercial antibodies against LPA_1, LPA_2, and LPA_4 proteins using full-length mouse or human (LPA_1 mouse to human, 97% identity; LPA_2 mouse to human, 84% identity) expression constructs overexpressed in HEK293 cells, wild-type (WT), and null mouse tissue lysates.

Most antibodies used for immunoblotting were not able to detect overexpressed mouse or human LPA_1, LPA_2, or LPA_4 proteins and moreover exhibited a strong background signal. No endogenously expressed proteins were recognized by most tested antibodies in different types of mouse tissue. Furthermore, the antibodies recognized cross-reactivity bands with other proteins in WT and LPA_1- or LPA_2-deficient KO protein lysates (data not shown). From seven existing commercially available antibodies, only one was specific for LPA_1, as shown in Figure 3A, C. Anti-LPA_2, which was generated and kindly donated by J. Aoki, was also specific (Figure 3A, C).

Both antibodies were shown to be sensitive, as they detected the LPA_1 or LPA_2 protein 1) when endogenously present in mouse brain protein lysates (Figure 3A, B), and 2) when fused to HA (HA-LPA_1 or HA-LPA_2) and overexpressed in HEK293 cells (Figure 3C). Specifically, western blot analysis showed bands between 55 and 35 kDa in native adult brain lysates and in HA-tagged human LPA_1 overexpressed in HEK293 cells lysate. The bands match the in silico predicted molecular weight of 41 kDa for LPA_1 (ExPASy; http://www.expasy.ch/tools) and were not detectable in brain lysates from LPA_1-KO mice (Figure 3A).

Immunoblot analyses for LPA_2 showed a dominant band pattern around 55 to 45 kDa and around 27 kDa in native brain lysate and were not detectable in brain lysates from LPA_2-KO mice (Figure 3A). The bands match the in silico predicted molecular weight of 39 kDa for LPA_2 (ExPASy; http://www.expasy.ch/tools).

To assess post-translational modification, N-glycosylation of both receptors was enzymatically removed by N-glycosidase F, and both antibodies were found to be sufficient to detect deglycosylated protein. Deglycosylation of LPA_1 produced a dominant band at 70 kDa and a new band around 30 kDa compared to glycosylated, endogenous protein (Figure 3B). For LPA_2, deglycosylation led to a clear shift, with bands detected between 55 and 27 kDa (Figure 3B). The immunoblots showed a different signal for overexpressed full-length HA-LPA_1 and

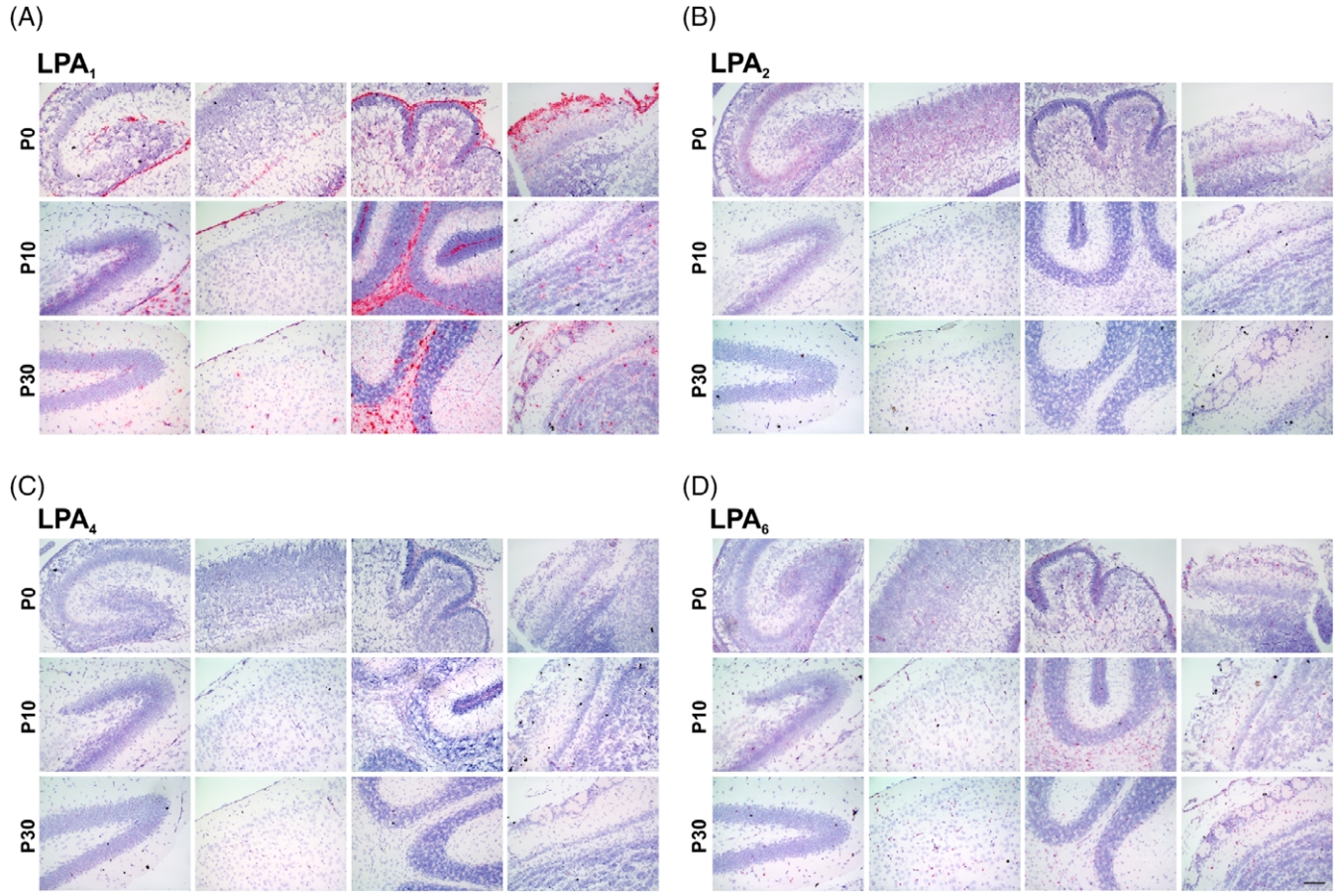

FIGURE 2 In situ hybridization of *LPA* receptors during mouse brain development. Analysis of *LPA1* (A), *LPA2* (B), *LPA4* (C), and *LPA6* (D) receptor mRNA expression at P0 (first row), P10 (second row), and P30 (third row) in hippocampus formation or dentate gyrus (first column), neocortex (second column), cerebellum (third column), and bulbus olfactorius (fourth column) is shown in red. Nuclei were counterstained with hematoxylin (blue). P, postnatal day. Scale bar = 100 μm

HA-LPA_2 compared to endogenous protein from mouse brain lysate. This band pattern could be explained as a consequence of post-translational modification of endogenous LPA_1 and LPA_2 receptors.

Additionally, anti-LPA_1 and anti-LPA_2 did not detect eGFP-LPA_4 fusion protein in immunoblotting, which was further evidence of the antibodies' specificity (Figure 3C).

Because we could not find a specific antibody for the LPA_4 receptor, we focused subsequent immunohistochemistry experiments on LPA_1 and LPA_2 receptors. To analyze the localization of LPA_1 (Figure 4) and LPA_2 (Figure 5) in mouse brain, we performed colocalization studies to determine cellular distribution of both receptors.

Western blot results on LPA_1 and LPA_2 antibody specificity were confirmed by immunostaining of WT and knockout (KO) brain sections, respectively, of P15 mice (Figures 4A and 5A). LPA_1 antibody showed strong staining of stem cells of the subgranular zone (SGZ) in the hippocampus, which was not detectable in KO brain sections (Figure 4A). Immunostaining with LPA_2 antibody was much weaker and showed diffuse background staining, but a punctuated pattern in soma of pyramidal neurons and proximal dendrites in the CA1 region of the hippocampus was clearly detectable and could not be shown in KO brain sections (Figure 5A).

The LPA_1 protein was barely observable in neuroblasts, expressing the class III β-tubulin (Tuj1) in P15 mouse cortex (Figure 4B). In contrast, LPA_2 receptor immunostaining revealed a clear colocalization in Tuj1-positive neuroblasts (Figure 5B), where the expression was detectable in cell bodies and extensions of cortical neurons (Figure 5B). Detailed immunohistochemistry analyses of LPA_1 and LPA_2 receptor expression in astrocytes has shown that both are expressed in the cell soma and in astrocyte processes (Figures 4C and 5C).

Additionally, we examined LPA_1 and LPA_2 protein expression in adult WT mice (Figures 4D and 5D). In accordance with qRT-PCR results, LPA_1 protein expression, as in P15, was strongly detectable in stem cells of the SGZ of the hippocampus and in white matter of the arbor vitae and molecular layer of the cerebellum of P60 WT mice, confirming the almost constant expression of LPA_1 during brain development (Figure 4D). LPA_2 protein was still detectable in P30 mice in

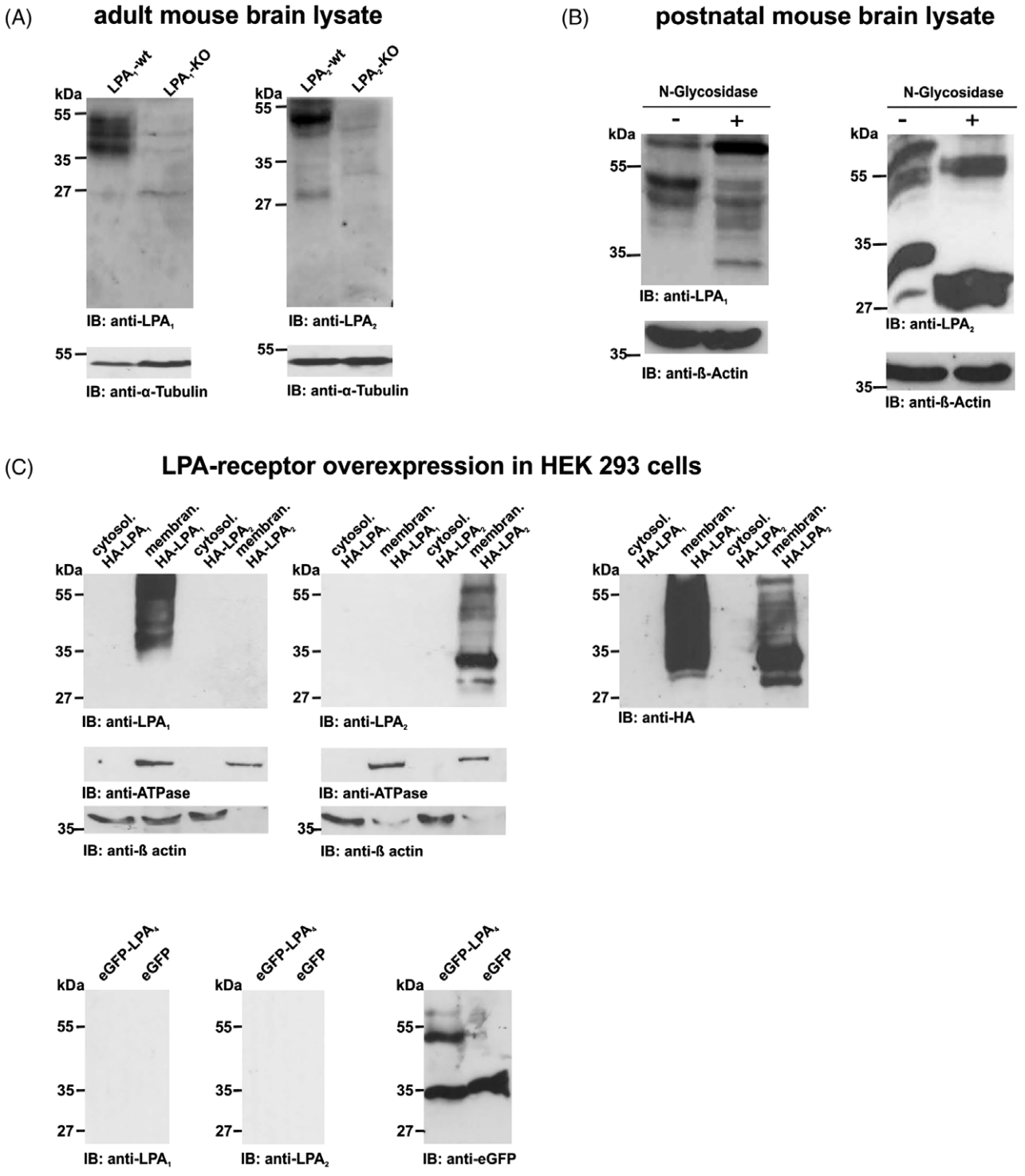

FIGURE 3 Specificity tests of anti-LPA1 and anti-LPA2. A: Whole brain lysates from LPA1-KO, LPA2-KO, and WT mice were separated on SDS-PAGE. One triple band between 55 and 35 kDa in WT mice exhibited anti-LPA1, whereas no band pattern was detectable in LPA1-KO lysates. Anti-LPA2 showed a dominant band pattern around 55 to 45 kDa and a weaker band around 27 kDa in WT, whereas no band pattern was detectable in LPA2-KO lysates. In conclusion, both LPA receptor antibodies were able to specifically recognize their endogenous mouse protein target. Alpha-tubulin was used as loading control. B: Postnatal mouse brain lysates were probed with anti-LPA1 or anti-LPA2 before and after incubation with N-glycosidase F. Deglycosylation of LPA1 led to a clear shift, with bands detected around 30 kDa. Endogenous glycosylated protein also showed an LPA1-positive band around 70 kDa. For LPA2, N-glycosidase F treatment resulted in a clear shift, with bands detected between 55 and 27 kDa. These results indicate N-glycosylation of both receptors. Beta-actin was used as loading control. C: Representative western blots of cytosol and membrane protein lysates from HEK293 cells overexpressing HA-LPA1, HA-LPA2, or eGFP-LPA4 constructs were used to exclude cross-reactions. Both antibodies also showed specificity to their target proteins in this test. Anti-HA, anti-GFP, and anti-ATPase were used as loading controls. KO, knockout, WT, wild-type

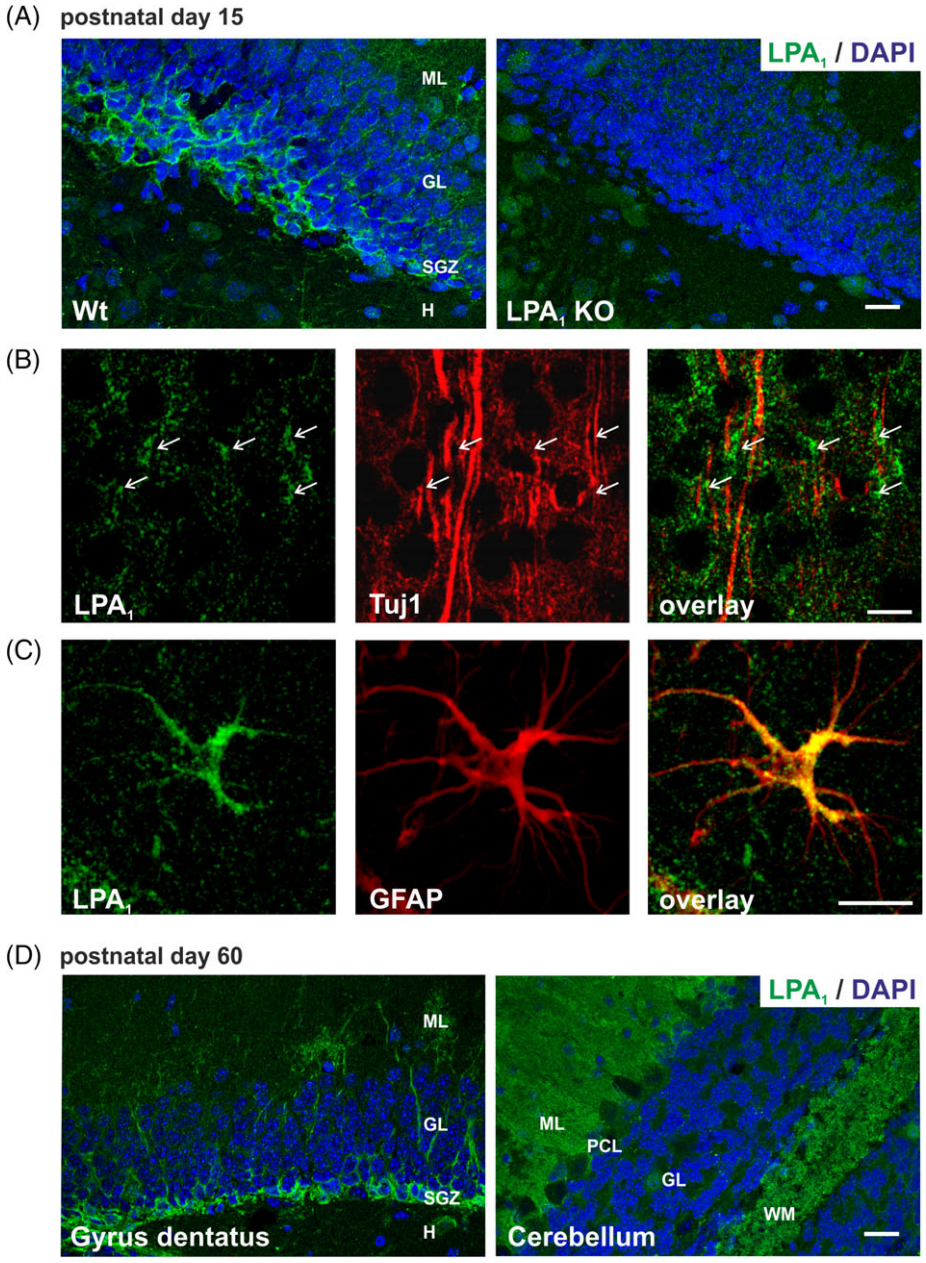

FIGURE 4 LPA1 receptor protein expression in mouse brain. A: LPA1 antibody specificity is verified by immunostaining of WT and LPA1 KO mice brains at P15. Representative confocal images of LPA1 (green) expression in WT dentate gyrus shows high LPA1 protein expression in neuroblasts of the SGZ, whereas staining is not detectable in KO mice. B: Neurons were visualized with the specific marker for postmitotic immature neurons Tuj1 (red). Cell bodies of neocortical neurons exhibited LPA1 receptor expression (green, arrows). C: Representative confocal image of LPA1 double-stained with the astrocyte marker GFAP (red). LPA1 receptor is expressed in the cell soma and in astrocyte processes. D: Representative confocal images of LPA1 (green) expression in mouse dentate gyrus and cerebellum at P60 is shown by immunohistochemistry. GL, granular layer; H, hilus; KO, knockout; ML, molecular layer; P, postnatal day; SGZ, subgranular zone; WM, white matter; WT, wild-type. Scale bars A,D = 20 μm. Scale bar C = 10 μm

soma and proximal dendrites of pyramidal neurons of CA1 hippocampal region and in Purkinje cells of the cerebellum (Figure 5D). However, the diffuse background staining and weak LPA_2 signal impeded explicit analysis of adult stages but confirmed the decrease of LPA_2 expression during maturation of the brain, which was shown by qRT-PCR.

2.4 | *LPA*$_1$, *LPA*$_2$, *LPA*$_4$, and *LPA*$_6$ receptors predominate and are dynamically expressed in brain cells

2.4.1 | Hippocampal neurons

To further specify the cellular abundance of *LPA*$_{1–6}$, we used qRT-PCR and ISH to analyze its expression in primary cultured brain cells (Figure 6A–F). We used hippocampal neurons after two days in vitro (2 DIV; *immature*). A cell at this maturation stage exhibits long neurites, one of which becomes the axon and elongates very rapidly, while the other neurites do not continue growing. Quantitative RT-PCR performed on young primary hippocampal neurons showed similar levels of *LPA*$_1$ and *LPA*$_2$ transcript expression (Figure 6A). These results corresponded to the *LPA* receptor expression in embryonic hippocampal tissue (Figure 1A). Furthermore, *LPA*$_4$ receptor expression was more than 10 times lower than that of *LPA*$_1$ and *LPA*$_2$, whereas *LPA*$_6$ was expressed 10 times higher. Additionally, expression of *LPA*$_3$ and *LPA*$_5$ in primary neurons was below detection. In hippocampal neurons of 14-day-old cultures (14 DIV; *mature*), when an extensive network of synaptic connections has been

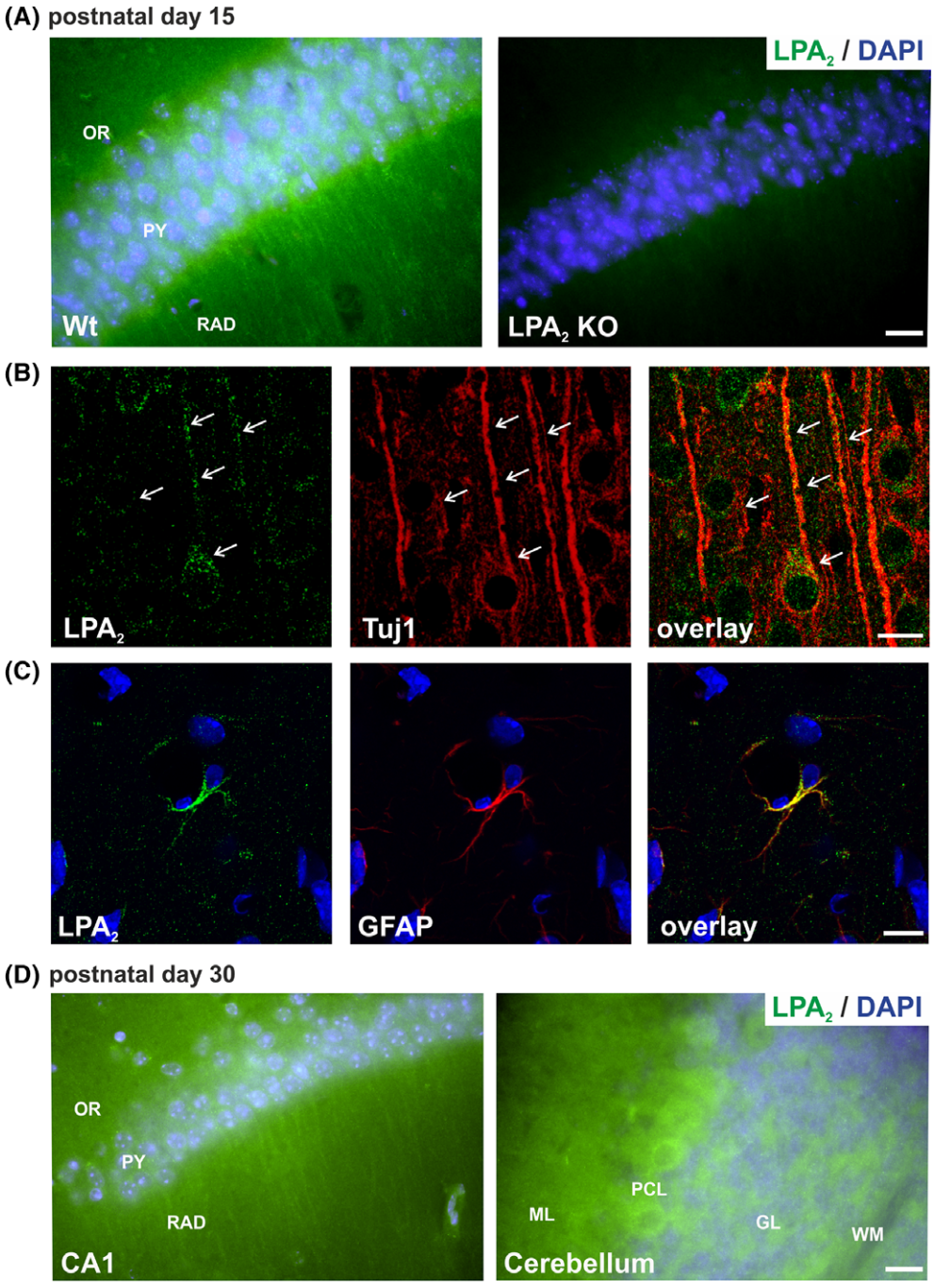

FIGURE 5 LPA2 receptor protein expression in mouse brain. A: LPA2 antibody specificity is verified by immunostaining of WT and LPA2 KO mice brains at P15. Representative fluorescence images of LPA2 (green) expression in WT CA1 region of the hippocampus shows punctuated LPA2 protein expression in somata and dendrites of pyramidal CA1 neurons, whereas staining is not detectable in KO mice. B: Neurons were visualized with the specific marker for postmitotic immature neurons Tuj1 (red). LPA2 receptor showed a signal in the extensions of Tuj1-positive neuroblasts (green, arrows). C: Representative confocal images of LPA2 double-stained with the astrocyte marker GFAP (red). LPA2 receptor is expressed in the cell soma and in astrocyte processes. D: Representative fluorescence images of LPA2 (green) expression in mouse CA1 hippocampal region and cerebellum at P30 is shown by immunohistochemistry. GL, granular layer; H, hilus; KO, knockout; ML, molecular layer; OR, striatum oriens; P, postnatal day; PY, striatum pyramidale; RAD, striatum radiale; SGZ, subgranular zone; WM, white matter; WT, wild-type. Scale bars A,D = 20 μm. Scale bar C = 10 μm

established, the LPA_1, LPA_2, and LPA_6 expression decreased, whereas the LPA_4 receptor decreased only slightly in comparison to immature neurons (Figure 6A). mRNA expression in hippocampal neurons was also confirmed by ISH experiments, where all four tested receptors were detected in the hippocampal formation of adult mice, as shown in the CA1 region in Figure 6B.

2.4.2 | Astrocytes and microglia cells

Expression of LPA_1 was more than 10-fold higher in primary astrocytes compared to microglia (Figure 6C). The amount of LPA_1 receptor expression in primary astrocytes was similar to the expression level in immature neurons (Figure 6A, B). However, the LPA_2 receptor expression was more than 10 times lower in astrocytes and microglia in comparison to neurons, as well as in comparison to LPA_1 expression in astrocytes (Figure 6C). LPA_4 receptor was detectable in astrocytes only at a low level (Figure 6C). Interestingly, the LPA_6 receptor shows similar expression level in astrocytes and microglia with a comparable expression level to mature neurons (Figure 6A–C). All four receptors were detectable by ISH in leptomeninges, indicating their additional non-neuronal expression in the brain (Figure 6D). Again,

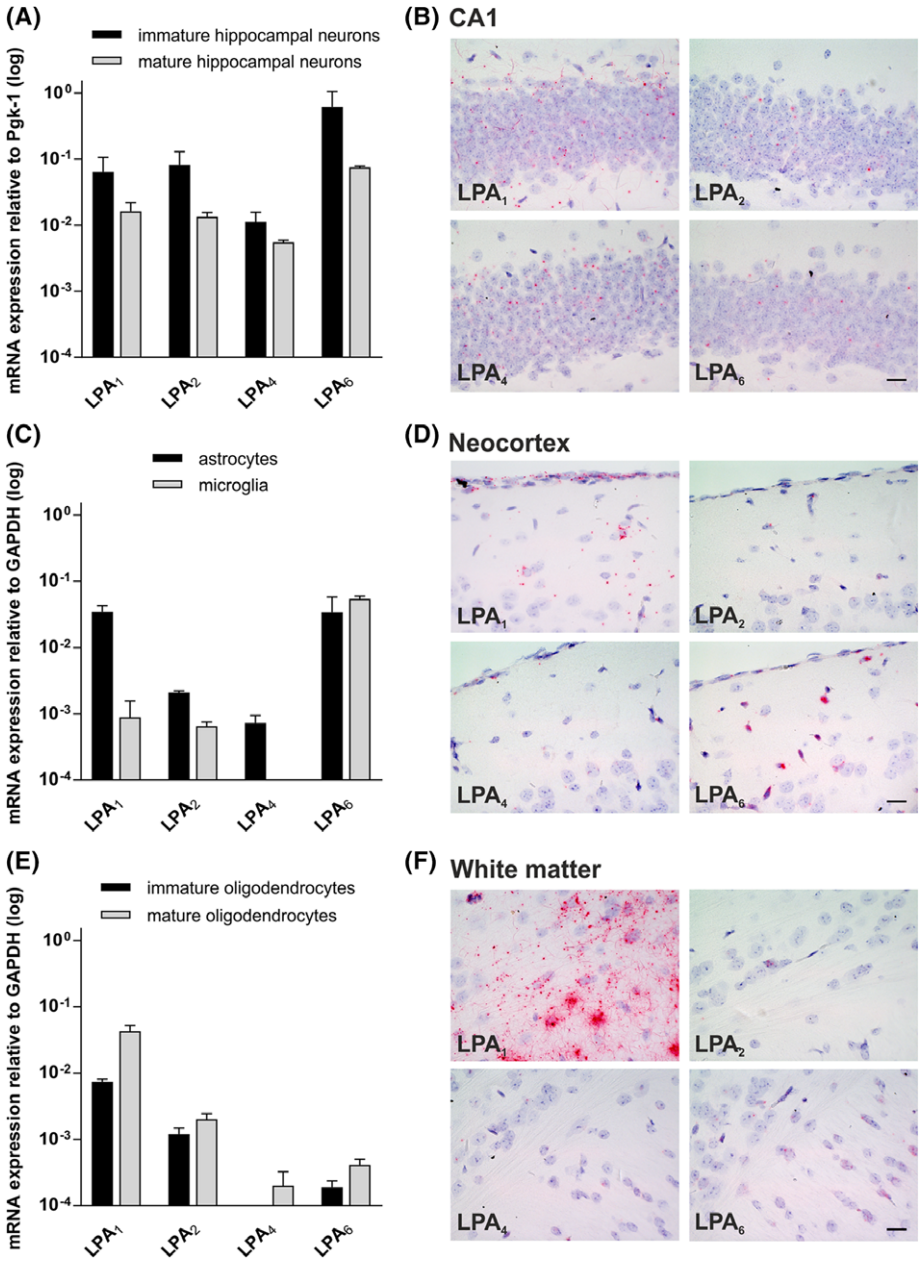

FIGURE 6 Gene expression profile of *LPA* receptors in brain cells. A: Quantitative RT-PCR of *LPA* receptor transcripts from immature (2 DIV) and mature (14 DIV) hippocampal neurons. qRT-PCR analysis reveals a robust expression of *LPA1*, *LPA2*, *LPA4,* and *LPA6* in both immature and mature neurons, whereas *LPA3* and *LPA5* were not detectable. The expression level of each receptor transcript for each sample was normalized to Pgk1. Error bars represent SD (n = 3). B: In situ hybridization of *LPA1*, *LPA2, LPA4*, and *LPA6* receptors in CA1 region of adult (P30) hippocampus. All receptors are expressed in the hippocampal formation in compact neuronal structures like the CA1 region. C: Quantitative RT-PCR of *LPA* receptor transcripts from primary astrocytes and microglia cells. In cultured primary astrocytes, *LPA1* and *LPA6* expression showed the highest transcript level, while *LPA2* and *LPA4* expression was more than 10 times lower. *LPA3* and *LPA5* were below detection level. In cultured primary microglia cells, only *LPA6* receptor shows a robust expression, whereas *LPA1* and *LPA2* mRNA expression was more than 10 times lower compared to *LPA6. LPA3, LPA4,* and *LPA5* were below detection level. The expression level of each receptor transcript for each sample was normalized to GAPDH. Error bars represent SD (n = 3). D: In situ hybridization of *LPA1*, *LPA2*, *LPA4,* and *LPA6* receptors in the adult (P30) neocortex. Here the receptors are also expressed in non-neuronal cells, like in leptomeninges covering the neocortex. E: Quantitative RT-PCR of *LPA* receptor transcripts from immature and mature oligodendrocytes. *LPA1*, *LPA2*, and *LPA6* receptor expression was detectable in immature oligodendrocytes. Here, *LPA1* shows the highest gene expression. In mature oligodendrocytes, *LPA1*, *LPA2*, *LPA4*, and *LPA6* gene expression was detected with a slight increase in expression level compared to immature oligodendrocytes. *LPA3* and *LPA5* expression were below detection level. The expression level of each receptor transcript for each sample was normalized to GAPDH. Error bars represent SD (n = 3). F: In situ hybridization of *LPA1*, *LPA2*, *LPA4*, and *LPA6* receptors in adult (P30) white matter regions of the corpus callosum. *LPA1* receptor mRNA is strongly expressed in white matter areas of the adult mouse brain. *LPA2*, *LPA4,* and *LPA6* receptor mRNA was detected with low signals in cells of the white matter region of the corpus callosum. DIV, days in vitro; P, postnatal day. Scale bars = 20 μm

expression of *LPA3* and *LPA5* in primary astrocytes and microglia cells was below detection.

2.4.3 | Oligodendrocytes

In primary immature and mature oligodendrocytes, *LPA1* receptor showed the highest expression in comparison to the other *LPA* receptors (Figure 6E), with an increase during maturation (Figure 6E). The *LPA2* receptor showed a 10-times-weaker expression level in comparison to *LPA1*, with a slight increase during maturation (Figure 6E). *LPA4* receptor was only detectable in mature oligodendrocytes at a very weak expression level. The *LPA6* receptor expression showed an increase in expression level during maturation, but at a very low expression level compared to *LPA1* and *LPA2*. ISH in white matter area of the corpus callosum of adult mice brain revealed very strong *LPA1* receptor mRNA expression and lower expression of *LPA2*, *LPA4*, and *LPA6* receptors (Figure 6F). Again, expression of *LPA3* and *LPA5* in primary astrocytes and microglia cells was below detection.

2.5 | Subcellular distribution of endogenous LPA_1 and LPA_2 receptor protein expression alters with neuronal maturation

Young hippocampal neurons showed typical formations at the tips of the axon where anti-ß-actin was used to visualize the cytoskeleton of growth cones (Figure 7A). Here, the LPA_1 receptor was detected as a dotted, weak signal all over the growth cone, from the center region (C-region) to the actin-rich peripheral region (P-region) (Figure 7A). The LPA_2 receptor was also located in the growth cones, but the signal was predominantly located in the C-region and not the periphery (Figure 7A). Interestingly, the protein distribution of LPA_1 and LPA_2 receptors was equal on the microtubule cytoskeleton, which turns into bundles aligned in parallel to form a nascent neurite shaft tipped by the growth cone (Figure 7A).

LPA_1 protein was not detectable in mature neurons when an extensive neuronal network had been established but was only observed in non-neuronal cells (Figure 7B). However, LPA_2 was clearly detectable in mature neuronal soma and weakly in dendrites, as shown by colocalization with the dendrite marker MAP2. Colocalization with the axonal marker Tau1 protein showed LPA_2 localization in the proximal axon segment (Figure 7B).

2.6 | Subcellular distribution of LPA_1 expression alters upon microtubule stabilization and destabilization

To mimic navigation processes of growth cones during neuronal polarization, we destabilized the microtubule network with nocodazole. Cells were incubated with nocodazole for five minutes and after removal further incubated in medium for 25 minutes. Right after the treatment, a lower LPA_1 expression in the P-region in comparison to untreated neurons was found (Figure 8A). After further 25 minutes without nocodazole (30 minutes), LPA_1 expression concentrated in the C-region. Hence, it shows that the treatment led to a decrease in growth cone size and a reduction of LPA_1 protein in the P-region. To mimic neuronal polarization, the microtubules of neurons were stabilized using Taxol. Taxol treatment led to a slightly changed distribution of LPA_1 receptors in the growth cone. After 15 minutes and 30 minutes, clusters of LPA_1 were found in the P-region of the growth cone (Figure 8A). Taxol was removed after 30 minutes and neurons were incubated in neuronal medium for an additional 30 minutes. At this time point (60 minutes), the LPA_1 signal was found in clusters in the P-region similar to the 30-minute time point (Figure 8A).

In comparison, destabilization of the growth cone by nocodazole did not affect the localization of LPA_2 (Figure 8B). The treatment did not induce any change in distribution of the receptor or the expression level. Even after the stabilization of the microtubules with Taxol, LPA_2 expression was found only in the C-region (Figure 8B). The distribution after this treatment resembles the LPA_2 expression in untreated neurons, where the receptor is also found only in the C-region of the growth cone (Figure 7A).

3 | DISCUSSION

We describe here the expression pattern of the six *LPA1–6* receptor genes in mouse brain from late embryonic developmental stage until adulthood. Our results show that during brain development, particularly when astrogenesis and oligodendrogenesis start and axons and dendrites continue to grow and mature, followed by synapse formation, maturation and stabilization, the LPA receptor genes are dynamically regulated in a temporal- and spatial-dependent manner.

3.1 | LPA receptor gene expression during brain development

Our data of *LPA1* receptor expression is in agreement with the results of others, which detected *LPA1* transcripts in whole-brain samples or neocortex of rodents from embryonic until adult stages in a biphasic expression pattern or increased during mouse brain development.[18,34] Our results revealed that *LPA1* mRNA is up-regulated, down-regulated, or biphasic-regulated during brain maturation depending on the analyzed mouse brain area.

The level of *LPA1* mRNA in the bulbus olfactorius was high in embryonic stages and down-regulated after birth. Genetic deletion of *LPA1* receptor has been reported as

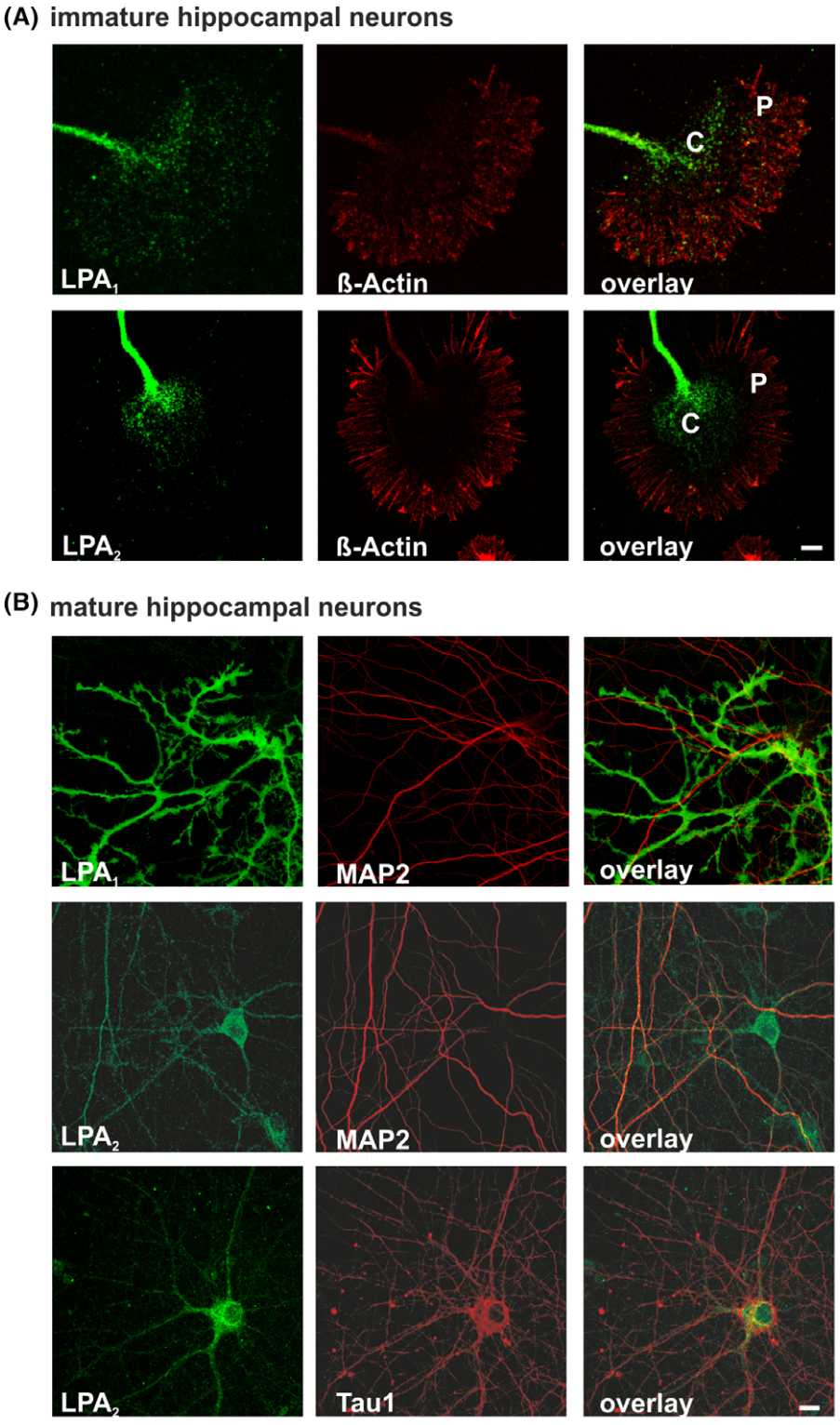

FIGURE 7 Subcellular distribution of LPA receptors in primary brain cells. Immunocytochemical analysis of endogenous *LPA1* and *LPA2* receptors within immature and mature neurons in vitro. A: Double-staining was prepared with anti-ß-actin (red) to visualize the cytoskeleton of a growth cone from hippocampal neurons cultured 2 DIV. *LPA1* (green) was detected all over the central region of the growth cone, as well as in the lamellipodia and filopodia. *LPA2* (green) was primarily located in the center of the growth cone. B: Representative confocal images of mature primary neurons cultured 14 DIV are shown. Cells were double-stained with the dendritic marker MAP2 (red) or axonal marker Tau1 (red). *LPA1* receptor (green) was not detectable in mature neurons but was detected strongly in non-neuronal cells. LPA2 receptor (green) was detected at neuronal cell bodies, weakly in MAP2-positive dendrites, but clearly in Tau1-positive axons. C, central region; DIV, days in vitro; P, peripheral region. Scale bars = 10 μm

associated with suckling defects,[14] which could explain the high expression in early stages that we observed.

Studies reporting *LPA1* expression in different brain cells vary in their findings during embryonic and postnatal development. Reports have shown *LPA1* expression in oligodendrocytes and astrocytes, as well as in neural progenitor cells (NPCs) in the ventricular zone but not in neurons.[16,19,22,50] Our staining in brain slices of postnatal mice showed a colocalization of LPA_1 with the astrocyte-specific marker protein glial fibrillary acidic protein (GFAP), and our qRT-PCR results demonstrated a high level of *LPA1* in cultured astrocytes and oligodendrocytes, whereas cultured microglia cells showed a moderate expression level. Interestingly, it has been shown that LPA-activated astrocytes can induce neuronal

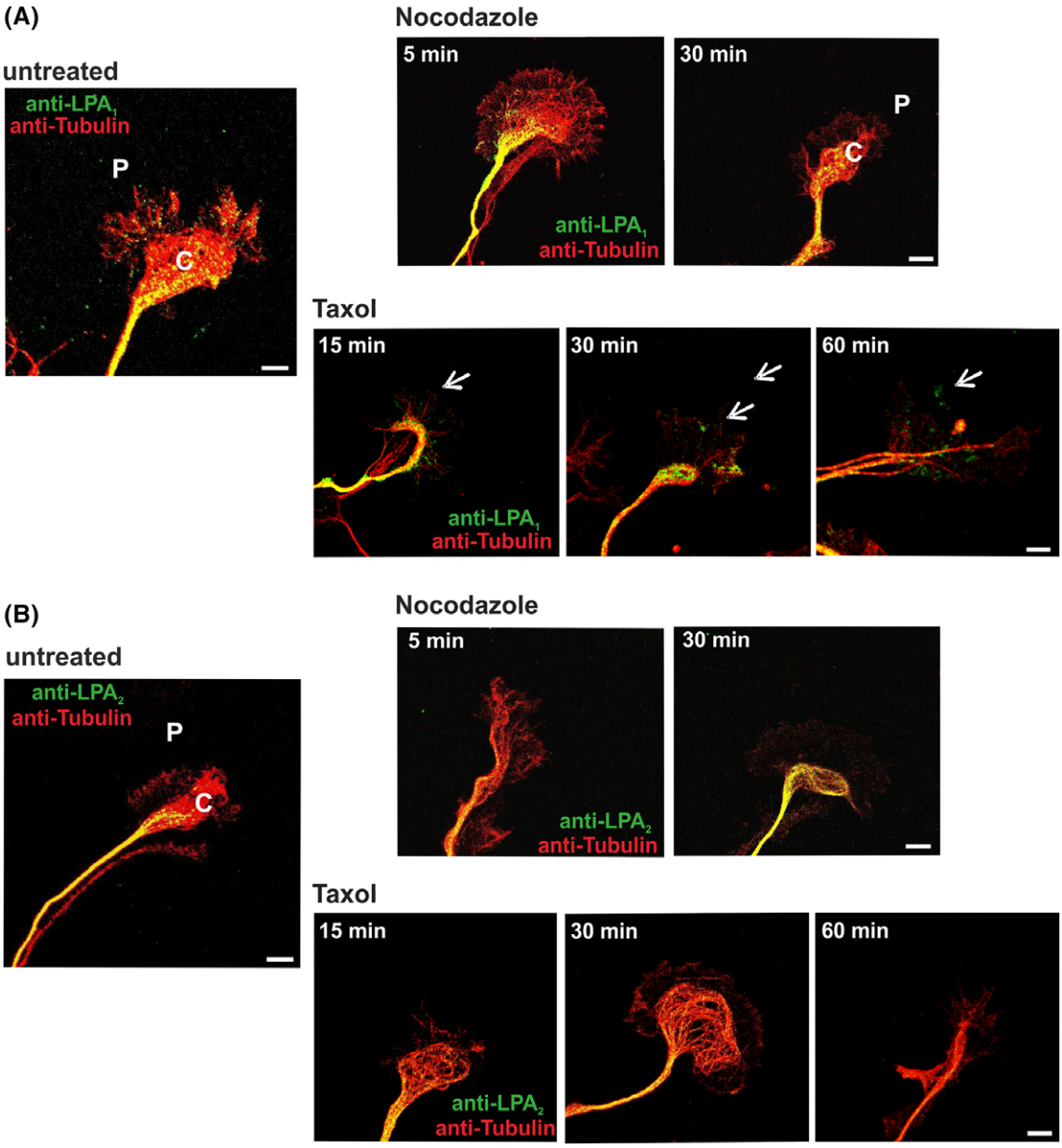

FIGURE 8 Localization analysis of LPA receptors upon stabilization/destabilization of microtubules. Immunocytochemical analysis of endogenous *LPA1* and *LPA2* receptors within immature neurons in vitro. Double-staining was prepared with anti-α-tubulin (red) to visualize the cytoskeleton of a growth cone from hippocampal neurons 2 DIV. A: *LPA1* (green) was detected in the central and peripheral regions prior to treatment. Treatment with nocodazole led to a restriction of LPA1 expression to the central region and a complete disappearance in the peripheral region. After 15 minutes, Taxol incubation first clusters away from the central region were seen. At the end of the treatment, clusters of *LPA1* were found in the peripheral region of the growth cone. Arrows indicate LPA1 clusters. B: In contrast, *LPA2* (green) was found only in the central region in untreated growth cones. No effect on the *LPA2* expression was observed after nocodazole or Taxol treatment. C, central region; DIV, days in vitro; P, peripheral region. Scale bars = 10 μm

differentiation and axonal outgrowth.[15,51] Moreover, nerve growth factor (NGF) production can also be enhanced by astrocytes' exposure to LPA.[52]

In oligodendrocytes it has been shown that extracellular LPA levels promote oligodendrocyte differentiation via an increase in Histone Deacetylase 1 and 2 (HDAC1/2) activity.[16] Two studies show predominant expression of LPA_1 and no expression of LPA_3 in microglia prepared from mouse brain.[53,54] In addition to LPA_1, we observed the expression of LPA_2 in cultured mouse microglia, unlike the reverse transcriptase experiments of Möller et al.[53] We also found predominant expression of LPA_6, which had not previously been tested.

Earlier studies of *LPA* receptor expression showed that LPA_1 had the highest expression level of all known LPA receptor genes, as determined by northern blot analyses of

human and mouse brain.[22,55] However, in our study, expression of the *LPA$_2$* receptor was equal to that of *LPA$_1$* and did not change significantly during hippocampal development. This lends weight to the importance of the *LPA$_2$* receptor during all stages in mouse brain development. Furthermore, this data is in line with published work from McGiffert et al, which shows diffuse expression of *LPA$_2$* receptor throughout the CNS.[56] Moreover, we could show a predominant expression of the *LPA$_2$* receptor in mature hippocampal neurons. This expression pattern differs from the *LPA$_1$* receptor and indicates the possible importance of the *LPA$_2$* receptor in neuronal networks. It is known that LPA promotes survival and differentiation of cortical precursor cells[12] and is involved in the regulation of adult hippocampal precursor cell proliferation and neurogenesis via activation of the AKT and MAPK pathways.[57]

Our qRT-PCR measurements of *LPA$_2$* expression in microglia also differed from previously published data. Whereas Möller et al[52] could not detect LPA_2 expression by reverse-transcriptase PCR in primary mouse microglia, we did observe *LPA$_2$* in these cells.

Several studies have analyzed *LPA$_3$* expression in tissue with various results. For example, as determined by northern blotting, Bandoh et al could not observe any *LPA$_3$* signal in human brain,[24] whereas another study detected *LPA$_3$* mRNA in several areas of the human forebrain, particularly the frontal cortex.[58] In contrast to the results from Contos et al, which showed *LPA$_3$* expression in the mouse brain by northern blot[59] and RT-PCR,[60] we could not detect mRNA transcripts of this receptor by qRT-PCR at any stage of brain development in the four analyzed brain areas. Previous investigation of assay efficiency and the correlation coefficient for the *LPA$_3$* receptor was about 0.95 to 0.99, providing that a data-interpretation error can be excluded.

Currently available data on *LPA$_4$* receptor expression shows a ubiquitous expression pattern in mouse tissue and particularly high levels in ovaries.[43,61,62] In all tested brain areas and development stages, *LPA$_4$* expression levels were much lower than those of *LPA$_1$*, *LPA$_2$*, and *LPA$_6$*. To date, no data is available on *LPA$_4$* expression in primary cells. By analyzing different primary cell types isolated from mouse brain, we found *LPA$_4$* in immature and mature neurons and astrocytes and at a low level in mature oligodendrocytes. LPA_4 protein is structurally distinct from classical LPA receptors and also binds G proteins. Currently, the physiological role of *LPA$_4$* receptor is poorly understood, and *LPA$_4$*-deficient mice display no apparent abnormalities.[61] Because specific antibodies for LPA_4 are not yet available, intracellular localization and localization studies in the brain have not been possible. Further analyses are required to understand the role of the LPA_4 receptor in the brain.

Our analysis proves the lack of *LPA$_5$* receptor expression in the brain. These results are in line with northern blot data from Lee et al.[26]

LPA_6 is the most recently identified member of the LPA receptor family.[63] It has been described that in *Xenopus,* the LPA_6 receptor is expressed in the developing telencephalon.[64] These results are in line with ours. We show that the *LPA$_6$* transcript is expressed higher than any other LPA receptor in all analyzed mouse brain area and development stages. Moreover, in primary neurons, immature and mature, astrocytes, and microglia we found a prominent *LPA$_6$* mRNA expression. Only oligodendrocytes, immature and mature, show only weak *LPA$_6$* expression. Especially in microglia, *LPA$_6$* receptor shows the highest expression of all LPA receptors. LPA exposure in primary murine microglia leads to a shift toward a proinflammatory M1-like phenotype.[65] The regulation of microglia polarization (eg, interference of the LPA signal transmission via LPA receptors) could represent a potential pharmacological target of neuroinflammation in the CNS.

Taken together, our expression analysis of *LPA* receptors throughout developmental and adult mouse brain demonstrated predominant expression of *LPA$_1$*, *LPA$_2$*, and *LPA$_6$* receptors, indicating a key player role during neuronal development and function. The lack of commercial antibodies specific for LPA receptors makes it difficult to study the expression pattern on protein level. Only one of three tested anti-LPA_1 antibodies was specific. The band pattern in the immunoblots correlated with published data by Cervera et al,[20] who generated a polyclonal antibody against a peptide on the C-terminus of LPA_1. No specificity was detected for two anti-LPA_2 and two anti-LPA_4 antibodies, which are commercially available.

The existence of several bands in the immunoblots points to a putative glycosylation of LPA_1 and LPA_2 receptors. Mouse LPA_1 has 364 AMino acids with an estimated molecular weight of ~41 kDa, whereas mouse LPA_2 consists of 348 AMino acids with an estimated molecular weight of ~39 kDa (ExPASy; http://www.expasy.ch/tools). Indeed, in silico analysis of the rat, mouse, and human LPA_1 or LPA_2 amino acid sequence (NetNGlyc 1.0; http://www.cbs.dtu.dk/services/) revealed a putative consensus N-glycosylation site of aa 27 and aa 35 for LPA_1, as well as aa 10 for LPA_2. N-glycosylation is the most common glycosylation in proteins, and analysis was done because it is an important post-translational modification with influence on the functional diversity as well as the activity of a protein. Furthermore, it provides stability for the protein and can affect oligomerization.[66,67] For Edg-1, a phospholipid receptor for sphingosine-1-phosphate, it has been shown that N-terminal glycosylation is important for ligand-induced internalization and receptor

dynamics within the membrane, proposing a similar influence for LPA receptors.[68]

3.2 | Subcellular localization of LPA_1 and LPA_2 receptors

For more detailed characterization of LPA receptors, we analyzed the localization of the proteins in primary cultured hippocampal neurons and brain slices. Based on our knowledge from the qRT-PCR data in primary neurons and the lack of an LPA_4 and LPA_6 antibody, we focused this study on LPA_1 and LPA_2 receptors alone.

In immature primary neurons, the localization of LPA_1 and LPA_2 receptors was especially interesting within the growth cones because the receptor ligand, LPA, has been described as inducing rapid growth cone collapse and neurite retraction in young postmitotic neurons and several cell lines, such as NG108-15, N1E-115, PC12, and SY-SH5Y.[17,22,69–78] Primary neurons form a number of immature neurites after plating in neuronal medium, which undergo random growth and retraction processes.[79] It is possible that LPA receptors are among other proteins involved in the regulation of such minor processes.

LPA_1 was not only detected in the C-region of growth cones, but also colocalized with actin-rich lamellipodia and filopodia. Previous studies of the LPA_1 homolog in *Xenopus* have shown, for example, that this protein plays a key role in the regulation of normal cortical actin assembly.[80] The involvement of LPA_1 in the rearrangement of actin, which is associated with ongoing neuronal polarization, has been shown multiple times.[17,81] The actin rearrangement induced through $G_{12/13}$ signaling is counteracted by G_q signals.[82] To control those processes, the presence of LPA receptors in the plasma membrane is important. This provides one explanation of LPA_1 clustering in the actin-rich P-region after Taxol treatment, corresponding to the mimicry of advanced polarization because, for example, constitutively active G_q can cause massive cell death in neurons.[82] However, further studies are required to confirm this hypothesis.

In contrast, LPA_2 was detected in the C-region but not in the P-region of growth cones. The C-region is thicker than the P-region and is thought to function as a terminal for vesicles and macromolecules transported along axonal microtubules.[83] Interruption of microtubule dynamics can lead to an abolition of vesicle migration, thus explaining the unchanged LPA_2 distribution during the stimulation experiments.[84] LPA_2 was described as a promoter of cell migration through interaction with the adhesion molecule TRIP6.[85,86] Localization of LPA_2 in the C-region of growth cones, an area where adhesion molecules are located, indicates the role of this receptor during neurite guiding. Furthermore, presynaptically located LPA_2 has been described as a player in regulation of the glutamatergic transmission.[87] LPA itself was shown to be an important phospholipid during early cortical development. It stimulates cell proliferation of cortical neuroblasts located in the ventricular zone of the cerebral cortex and inhibits neuronal differentiation in the cortical plate.[88] Because postmitotic neurons produce LPA, a reciprocal control mechanism may regulate cell proliferation, dendritic outgrowth, and differentiation in these two cortical layers. Our data on primary hippocampal neurons in vitro show localization of LPA_1 and LPA_2 receptors in growth cones and may hint at a role in axonal and/or dendritic outgrowth and guidance in the hippocampus. Confirming this approach could be based on LPA_1 and LPA_2 receptor expression data in vivo of developmental hippocampus.

The localization pattern of these receptors differs in mature hippocampal neurons in culture compared to immature neurons in that the LPA_1 receptor could no longer be detected in differentiated neurons. Additionally, LPA_1 was hardly detected in neurons in brain slices, but instead in GFAP-positive astrocytes. The localization of LPA_2 was homogeneously distributed in cell body of mature neurons and Tau1-positive axons. This expression pattern was in line with LPA_2 staining in brain slices of postnatal mice.

4 | CONCLUSION

In this study, we found development-dependent expression of LPA receptors in mouse brain and in cultured hippocampal primary neurons. In view of the complex expression patterns of LPA receptors within organisms, further physiological and pathophysiological function of LPA signaling remains to be characterized. Currently, six receptors have been identified as specific G protein–coupled receptors for LPA. Recent publications have suggested that three additional receptors, GPR87, GPR35, and P2Y10, may be responsive to LPA.[89–93] Although further study is required to confirm these observations, it is clear that LPA signaling and LPA receptor expression are very complex. Thus, many more physiological and pathophysiological functions of LPA signaling remain to be revealed and characterized.

5 | EXPERIMENTAL PROCEDURES

5.1 | Animals

For all experiments, timed-pregnant, postnatal, and adult WT C57BL/6 or BALB/c and LPA_1-KO or LPA_2-KO mice were obtained from Charité–Universitätsmedizin central animal facility (FEM), the central animal facility of the University Medical Center Rostock, or the central animal facility of the Carl von Ossietzky University Oldenburg and were kept under standard laboratory conditions (12-hour light/dark cycle; 55% +/−15% humidity; 22°C +/− 2°C RT, and water ad libitum, enriched and grouped) in accordance with German and European guidelines (2010/63/EU) for the use of laboratory

animals. Approval of experiments was obtained from the local ethics body of Berlin (LAGeSO: T0108/11). For experiments, the day of the vaginal plug following mating was designated E0.5. Experiments were performed on E16, E18, and E19 embryos and perinatal pubs (P0, P5, P10, P15, P20, and P30); 4- and 8-week-old male mice were used for protein extraction. Generation and characterization of mice with LPA_1- and LPA_2-receptor deficiency have been described previously.[14,94]

5.2 | Primary mouse hippocampal neuron cultures

Primary hippocampal neurons were prepared from E18 (+/−0.5 day) mouse embryos as described previously.[95] The cells were cultured on poly-L-lysine–coated glass coverslips in Neurobasal A medium supplemented with 2% B27, 0.5 mM glutamine (Gibco-Invitrogen, Basel, Switzerland), and the antibiotics penicillin and streptomycin (100 U/mL PAN-Biotech, Aidenbach, Germany). Neurons were plated at a density of 2.1×10^4 cells/cm^2 and were routinely maintained at 37°C and 5% CO_2.

5.3 | Primary mouse astrocyte and microglia cultures

For astrocyte and microglia preparation, neocortex and cerebellum from mouse pups aged P0 to P2 were isolated.[34] The tissue was washed in Dulbecco's Modified Eagle's Medium (DMEM, Gibco-Invitrogen, Basel, Switzerland) 4.5 g/L glucose containing 10% fetal calf serum (FCS, PAN-Biotech, Aidenbach, Germany), 200 mM glutamine, and 100 U/mL penicillin/streptomycin, then underwent careful homogenization with a fire-polished Pasteur pipette and centrifugation at 300 × g and 4°C for one minute. The supernatant was transferred into a new tube, homogenized again, and centrifuged for five minutes at 1200 × g and 4°C. The pellet was re-suspended in fresh medium and plated in culture flasks, which had been pre-coated with poly-L-lysine. The cells were incubated at 37°C with 5 %CO_2. After two days, the medium was refreshed and the cells were allowed to continue incubating until most of the microglia had detached from the astrocytes. To remove the remaining attached microglia, the cells were shaken for two hours at 37°C. Afterward, the supernatant was plated again in culture medium containing 2% FCS. The astrocytes still attached to the bottom of the culture flask were used for further experiments after 14 to 16 days.

5.4 | Primary mouse oligodendrocyte cultures

Oligodendrocytes were prepared after an adapted protocol from Chen et al.[96] Briefly, the cerebral hemisphere of each mouse at P5 was dissected and then digested with papain (100 U, Worthington Biochemical Corporation) by gentle trituration. The cell suspension from three mice was seeded to a poly-D-lysine (100 µg/mL in phosphate-buffered saline (PBS), Sigma, St. Louis, MO, USA) -coated T75 flask and maintained in DMEM high-glucose medium (Invitrogen, Carlsbad, CA, USA) supplemented with 20% fetal bovine serum (Thermo Fisher, Waltham, MA, USA) and 1× penicillin/streptomycin. After 24 hours, the medium was changed completely, then half of the medium was replaced every three days. Insulin (5 µg/mL, Sigma, St. Louis, MO, USA) was added at DIV 7. At DIV 10, oligodendrocyte progenitor cells (OPCs) were detached from the mixed glial culture by differential shaking (sequentially with 75 rpm for 1 hour and 220 rpm for 16 hours) and purified by adhesion to uncoated Petri dishes. About 200 000 purified cells were seeded into each well of a poly-D-lysine-coated six-well plate and cultured in Maltose-Yeast Extract-Malt Extract (MYM) medium, which contains DMEM high-glucose medium, sodium pyruvate, L-glutamine, B27 supplement (all from Invitrogen, Carlsbad, CA, USA), insulin, transferrin, putrescine, progesterone, sodium selenite, T3, hydrocortisone, biotin, vitamin B12 (all from Sigma, St. Louis, MO, USA), and ceruloplasmin (Calbiochem, Merck, Darmstadt, Germany).[97] OPCs simultaneously differentiate into oligodendrocytes in the absence of mitogens, such as platelet-derived growth factor (PDGF) and basic fibroblast growth factor (bFGF).[98] The cells were cultivated without changing the medium and immature oligodendrocytes were collected after three days, mature ones after six days.

5.5 | Cell culture, transfection, and protein extraction

HEK293 cells were routinely maintained at 37°C and 5% CO_2 in DMEM supplemented with 10% FCS, 200 mM glutamine, and 100 U/mL penicillin/streptomycin. HEK293 cells were transfected transiently with N-terminal, HA-tagged human LPA_1 and LPA_2 (in pcDNA3, Invitrogen, Carlsbad, CA, USA) or N-terminal, eGFP-tagged mouse LPA_4 receptor (in pEGFP-C1, BD Biosciences, Palo Alto, CA, USA). For transfection, cells were seeded at a density of 3×10^4 cells/cm^2 on poly-L-lysine–coated cell culture plates overnight. On the following day, the culture medium was refreshed and 0.52 µg plasmid-DNA was diluted in 45 µL water, 4 µL $CaCl_2$ (2.5 M), and 45 µL HEPES buffer (pH 7.1–7.2). Volume and DNA concentration were calculated to an area of 10 cm^2 from the cell culture plate. The transfection complexes were added to the cells, and cells were cultured at 37°C and 5% CO_2 for at least 24 hours. For protein extraction, cells were lysed in lysis buffer (20 mM Tris, pH 7.5, 0.25 M sucrose, 1 mM EGTA, 5 mM EDTA, 25× proteinase inhibitor cocktail from Sigma, St. Louis, MO, USA) and centrifuged for 10 minutes at 13.000 g. The supernatant was replaced and

stored at −20°C. For membrane protein isolation, the cells were centrifuged at 150.000 × g for 30 minutes at 4°C. The resulting supernatant held the cytosolic protein fraction and was stored at −20°C. The pellet was re-suspended in 100 µL lysis buffer and 0.1% Triton X-100. After further incubation for 30 minutes on ice, it was centrifuged again for five minutes at 5000 × g at 4°C. The supernatant, now containing the membrane proteins, was replaced and stored at −20°C.

5.6 | Deglycosylation

100 µg protein, 1 µL 25% SDS, and 1 µL ß-mercaptoethanol (1:50) were boiled for 15 minutes at 65°C. Afterward, 5 µL N-glycosidase F (5 U) or 5 µL 20 mM Tris (control) were added and incubated at 37°C overnight. 1 µL additional ß-mercaptoethanol and protein sample buffer were added and an SDS-PAGE with subsequent western blot and immunodetection were performed.

5.7 | Immunocytochemistry

Cultured primary neurons were fixed in ice cold 4% paraformaldehyde (PFA) in 1x PBS containing 15% sucrose for 20 minutes at room temperature (RT) and subsequently permeabilized with 0.1% Triton X-100 and 0.1% sodium citrate in 1x PBS for three minutes at 4°C. Cells were then incubated for two hours at RT in 10% FCS in 1x PBS (PBSF). For stabilization or destabilization studies, the neurons were treated with 100 nM Taxol or 500 nM nocodazole (both from Sigma, St. Louis, MO, USA), respectively, in Hank's Buffered Salt Solution (HBSS, Thermo Fisher, Waltham, MA, USA) for up to 60 minutes. Drug concentration and duration of treatment were adjusted after Witte et al.[99] After removal of the medium at the indicated time points (5, 15, 30 or 60 minutes) and washing with 1× PBS, cells were fixed in ice cold 4% PFA in 1× PBS containing 15% sucrose for five minutes at RT. At this point cells were kept in 1x PBS to allow synchronization of all wells. Following washing with 1× PBS, they were permeabilized with 0.2% Triton X-100 in 1× PBS for 10 minutes at RT. Subsequently, cells were incubated with 20% FCS in 1x PBS for two hours at RT. All neurons were stained with polyclonal anti-LPA_1 1:500 (Cayman Chemical, Ann Arbor, MI, USA) or monoclonal anti-LPA_2 at 1:250 (generated by J. Aoki), each combined with either monoclonal anti-ß-actin 1:500 or monoclonal anti-MAP2, both diluted to 1:1000 (Sigma, St. Louis, MO, USA), monoclonal anti-Tau1 at 1:200 (Millipore, Billerica, MA, USA) or monoclonal anti-α-Tubulin (1:500, Sigma, St. Louis, MO, USA). All primary antibodies were diluted in PBSF and incubated overnight at RT. Goat anti-rabbit 488 or goat anti-rat 488 and goat anti-mouse 568 Alexa Fluor conjugated (1:1000; Molecular Probes, Eugene, OR, USA) secondary antibodies were diluted in PBSF and incubated at RT for one hour. Coverslips were mounted on slides with Immu-Mount and used for microscopy.

5.8 | Immunohistochemistry

C57BL/6, LPA_1-KO, and LPA_2-KO mice at P15, P30, and P60 were deeply anesthetized with a mixture containing ketamine (Pfizer, Karlsruhe, Germany) and xylazine (Rompun, Bayer HealthCare, Leverkusen, Germany), or with sodium pentobarbital (Narcoren, Boehringer Ingelheim, Germany), then transcardially perfused with 0.9 M NaCl solution, followed by 4% PFA in 0.1 M sodium phosphate buffer (PB) (pH 7.2). Brains were removed and stored in fixative for one to two days at 4°C. Coronal and sagittal brain vibratome sections (35–50 µm) were prepared. For background fluorescence reduction, slices were treated with 1% $NaBH_4$ in PB for 15 minutes at RT with mild agitation. After four washing steps with PB, slices were incubated for one hour at RT with blocking solution: 10% FCS, 1% normal goat serum (NGS, Vector laboratoiers, Burlingame, CA, USA) 0.1% glycine, 0.1% lysine, and 0.1% Triton X-100 in PB. Subsequent primary antibody incubation was carried out in the same solution overnight at 4°C with antibodies against LPA_1 (1:200 to 1:500, Cayman Chemical, Ann Arbor, MI, USA) or LPA_2 (1:100 to 1:250, generated by J. Aoki) and against GFAP, an astrocyte marker (1:500, Millipore, Billerica, MA, USA), or Tuj1, a neuroblast marker (1:500, Covance, Princeton, NJ, USA). After three washing steps with PB, slices were incubated with goat anti-rabbit 488 or goat anti-rat 488 and goat anti-mouse 568 Alexa Fluor conjugated antibodies (1:1000; Molecular Probes, Eugene, OR, USA) in blocking solution (without Triton X-100) overnight at 4°C for two hours at RT. Finally, brain slices were washed three times and coverslipped with Immu-Mount (Thermo Fisher Scientific, Waltham, MA, USA) for further microscopic analysis.

5.9 | Microscopy

Brightfield images of ISH and fluorescence images of immunohistochemical stainings of brain slices were captured with an IX83 inverted imaging system with a DP80 camera (Olympus, Shinjuku, Japan). Images were taken with either 20× UPlanSApo (0.75 NA) or 60× UPlanSApo (oil-immersion, 1.35 NA) objectives. Confocal images of primary neurons and brain slices were acquired with upright laser microscopes (Leica DM 2500 and Leica SP8, Leica Microsystems, Wetzlar, Germany) equipped with a 63× objective (oil-immersion, 1.2 NA) using sequential scanning with the 488-nm line of an argon-ion laser and the 543-nm line from helium-neon lasers (for Alexa 488 and Alexa 568, respectively). Background correction and adjustment of brightness and contrast were performed using either Leica confocal software (Leica Microsystems, Wetzlar, Germany), cellSens

software (Olympus, Shinjuku, Japan), or ImageJ (NIH, Bethesda, MD, USA).

5.10 | Quantitative real-time PCR

C57BL/6 mice at different ages (E16–P30) were used for total RNA purification. The neocortex, hippocampus, cerebellum, and bulbus olfactorius were dissected and immediately snap-frozen following harvesting from three sets of six animals of each age. The tissue was subsequently homogenized in TRIzol (Thermo Fisher Scientific, Waltham, MA, USA) reagent. Primary neurons, astrocytes, and microglia cells (approximately 3×10^5 cells for each experiment from three independent preparations of three pregnant animals) were scraped in 1× PBS and centrifuged for five minutes at 900 × g at 4°C. Cell pellets were dissolved in 1 mL TRIzol reagent (Invitrogen, Eugene, OR), and the total RNA was purified according to the TRIzol protocol. RNA concentrations were determined using a UV/Vis spectrophotometer (Biomate 3 spectrophotometer, Thermo Fisher Scientific, Waltham, MA, USA). Subsequently, 2.5 µg total RNA was reverse-transcribed to single-stranded cDNA using the commercially available High-Capacity cDNA Reverse Transcription Kit (Applied Biosystems, Foster City, CA, USA) according to the manufacturer's instructions. As a control, reaction was performed without MultiScribe reverse transcriptase. The quality of the amplified cDNA (with and without MultiScribe reverse transcriptase) was controlled by ß-actin PCR.

The TaqMan Universal PCR Master Mix Kit was used for the TaqMan assay, and the reactions were performed in a 96-well optical reaction plate from Applied Biosystems (Foster City, CA, USA). The following gene expression assays were employed: for LPA_1 (assay ID: Mm00439145_m1), LPA_2 (assay ID: Mm00469562_m1), LPA_3 (assay ID: Mm01312593_m1), LPA_4 (assay ID: Mm01228533_m1), LPA_5 (assay ID: Mm01190818_m1), and LPA_6 (assay ID: Mm00613050_s1 und Mm00519013_s1). GAPDH (glyceraldehyde-3-phosphate dehydrogenase, part no.: 4352932E), Pgk-1 (phosphoglycerate kinase 1, assay ID: Mm00435617_m1), and HPRT (hypoxanthine guanine phosphoribosyl transferase, forward 5-ATCATTATGCCGAGGATTTGGAA-3; reverse 5-TTGAGCACACAGAGGGCCA-3; probe 5-TGGACAGGACTGAAAGACTTGCTCGAGATG-3, Metabion, Planegg, Germany) were used as internal controls to confirm the successful extraction of RNA, conversion to cDNA, and qRT-PCR reaction. To determine the linear relationship between the threshold cycle (Ct) and the log starting copy number, serial dilutions of cDNA were amplified. In all experiments, the correlation coefficient was between 0.95 and 0.99. As a template for LPA_1, LPA_2, LPA_4, and LPA_6 assays, hippocampus cDNA was used; for LPA_3 and LPA_5 assays, spleen cDNA was used. To determine the relative gene expression in each experiment, samples were double-tested and one "no template" control (NTC) was used. Quantitative RT-PCR was mainly carried out using the ABI PRISM 7700 Sequence Detection System; only for analysis of oligodendrocytes, the ViiA 7 Real-Time PCR System was used (both from Applied Biosystems, Foster City, CA, USA). The identity and purity of primary cells were shown by qRT- PCR with the neuroblast-specific class III β-tubulin (Tuj1) as a marker for neurons, the glial fibrillary acidic protein (GFAP) as a marker for astrocytes, the ionized calcium-binding adaptor molecule 1 (Iba1) as a marker for microglial cells, the neuron-glial antigen 2 (NG2) as a marker for immature oligodendrocytes, and the myelin basic protein (MBP) as a marker for mature oligodendrocytes (data not shown). All controls were included for all experimental time points (RNA quality, cDNA quantity and quality, qRT-PCR quality) and each experimental sample, and were always negative.

5.11 | In situ hybridization

ISH was performed on formalin-fixed 8-µm paraffin sections using the Advanced Cell Diagnostics RNAscope 2.5 HD Detection Kit (Bio-Techne, Minneapolis, MI, USA). Briefly, C57Bl/6 mice were sacrificed by cervical dislocation, and brains were dissected and immersion-fixed with 10% neutral buffered formaline for 16 to 32 hours at 4°C. Brains were dehydrated using a standard ethanol series, followed by xylene. Paraffin embedding was carried out overnight and 8-µm sections were prepared with a sliding microtome. Sections were mounted on Superfrost Plus adhesion microscope slides (Thermo Fisher Scientific, Waltham, MA, USA) and dried overnight at RT. Brain sections were incubated with boiling target retrieval buffer for 15 minutes and then treated with protease plus for 30 minutes. Hybridization was performed following the manufacturer's protocol. The probes are as follows: Lpar1 (no. 318591), Lpar2 (no. 442691), Lpar4 (no. 318341), Lpar6 (no. 318351), and DapB (negative control). Nuclei were counterstained with hematoxylin.

5.12 | Data Analysis

For quantitative comparison of the LPA receptor gene expression, data extracted from each qRT-PCR run was analyzed using the 7500 Fast system software and the QuantStudio Real-Time PCR software (both from Applied Biosystems, Foster City, CA, USA). The value of the noise fluorescence, usually indicated as the baseline of the run, was automatically determined. The Ct was automatically calculated and used to quantify the starting copy number of the target mRNA. Normalization of LPA receptor genes in brain tissue, astrocytes, microglia cells, and oligodendrocytes was evaluated to internal control of GAPDH and HPRT expression by means of the 2-dCt method.[100] Normalization of

LPA gene expression in primary neurons was carried out in addition to internal control of Pgk-1 using the same method.

5.13 | Western blot analysis

Protein samples for western blots were obtained from whole brain of BalbC WT, LPA_1-KO, and LPA_2-KO mice. Tissue was homogenized in lysis buffer comprising 10 mM Tris-HCl, pH 7.4, 10 mM EDTA, 1 mM phenylmethylsulfonyl fluoride, 1 µg/mL pepstatin A, 1 µg/mL leupeptin, 10 µg/mL soybean trypsin inhibitor, and 25 mM glycerophosphate as described.[101] Afterward, the lysates were centrifuged for 10 minutes at 14.000 × g and 4°C. Protein extracts (40 µg) were boiled for 15 minutes at 60°C and separated on a 12% SDS-gel. Blotting was carried out with nitrocellulose membrane BA 85 (Whatman, Maidstone, UK) using a Semi-Dry Electro Blotter (PEQLAB, VWR International, Radnor, PA, USA) for 50 minutes at 14 V. Membranes were blocked for at least 1 hour at RT in 1× PBS buffer with 0.05% Tween 20 and 10% skim milk. The membranes were first incubated with anti-LPA_1 (1:500) or anti-LPA_2 (1:500) overnight at 4°C in the same buffer. Protein detection from LPA receptors overexpressing HEK293 cells lysate was carried out with anti-HA, clone 3F10 (1:1000) (Roche Applied Science, Penzberg, Germany), or anti-GFP (1:2000) (Abcam, Cambridge, UK). After washing three times with 1× Tris-buffered saline (TBS) with 0.05% Tween20, membranes were incubated with secondary horseradish peroxidase conjugated antibody (1:5000, anti-rabbit IgG or anti-rat IgG) (GE Healthcare, Chicago, IL, USA) in 1× TBS, 0.05% Tween 20 overnight at 4°C. After washing, the immunoreaction was visualized using Pierce ECL Western Blotting Substrate on CL-XPosure films. After exposure, the procedure of immunodetection was repeated, starting with blocking. Anti-ß-tubulin (1:2500) (Synaptic Systems, Göttingen, Germany), anti-ß-actin (1:20.000) (Sigma, St. Louis, MO, USA), or anti-ATPase (1:500) (Abcam, Cambridge, UK) was incubated for 1 hour at RT in 1× TBS, 0.05% Tween 20; anti-mouse IgG (1:5000) (GE Healthcare, Chicago, IL, USA) served as secondary antibody.

Other tested and not specific antibodies for immunodetection were rabbit polyclonal anti-LPA_1 (GeneTex Inc., Irvine, CA, USA), rabbit polyclonal anti-LPA_1 (LifeSpan Biosciences, Seattle, WA), rabbit polyclonal anti-LPA_2 (Novus Biologicals, Littleton, CO, USA), rabbit polyclonal anti-LPA_2 (Abgent, Heidelberg, Germany), rabbit polyclonal anti-LPA_4 (Acris Antibodies, Herford, Germany), and rabbit polyclonal anti-LPA_4 (Abcam, Cambridge, UK).

ACKNOWLEDGMENTS

Bettina Brokowski, Rike Dannenberg, Nora Ebermann, Kerstin Kleinschmidt, Robin Piecha, and Jan Csupor are acknowledged for their excellent technical assistance. The authors thank Jutta Schüler for help with the confocal analyses, and James Ari Liebkowsky for editing the article.

CONFLICT OF INTEREST

The authors declare that they have no competing interests.

ORCID

Anja U. Bräuer https://orcid.org/0000-0003-3651-1470

REFERENCES

1. Fukushima N, Weiner JA, Chun J. Lysophosphatidic acid (LPA) is a novel extracellular regulator of cortical neuroblast morphology. *Dev Biol*. 2000;228:6-18.
2. Tokumura A. Metabolic pathways and physiological and pathological significances of lysolipid phosphate mediators. *J Cell Biochem*. 2004;92:869-881.
3. Choi JW, Chun J. Lysophospholipids and their receptors in the central nervous system. *Biochim Biophys Acta*. 1831;2013:20-32.
4. Yung YC, Stoddard NC, Chun J. LPA receptor signaling: pharmacology, physiology, and pathophysiology. *J Lipid Res*. 2014;55:1192-1214.
5. Steiner MR, Urso JR, Klein J, Steiner SM. Multiple astrocyte responses to lysophosphatidic acids. *Biochim Biophys Acta*. 2002;1582:154-160.
6. Rao TS, Lariosa-Willingham KD, Lin FF, et al. Pharmacological characterization of lysophospholipid receptor signal transduction pathways in rat cerebrocortical astrocytes. *Brain Res*. 2003;990:182-194.
7. Dubin AE, Herr DR, Chun J. Diversity of lysophosphatidic acid receptor-mediated intracellular calcium signaling in early cortical neurogenesis. *J Neurosci*. 2010;30:7300-7309.
8. Campbell DS, Holt CE. Chemotropic responses of retinal growth cones mediated by rapid local protein synthesis and degradation. *Neuron*. 2001;32:1013-1026.
9. Yuan XB, Jin M, Xu X, et al. Signalling and crosstalk of Rho GTPases in mediating axon guidance. *Nat Cell Biol*. 2003;5:38-45.
10. Fincher J, Whiteneck C, Birgbauer E. G-protein-coupled receptor cell signaling pathways mediating embryonic chick retinal growth cone collapse induced by lysophosphatidic acid and sphingosine-1-phosphate. *Dev Neurosci*. 2014;36:443-453.
11. Holtsberg FW, Steiner MR, Keller JN, Mark RJ, Mattson MP, Steiner SM. Lysophosphatidic acid induces necrosis and apoptosis in hippocampal neurons. *J Neurochem*. 1998;70:66-76.
12. Kingsbury MA, Rehen SK, Contos JJ, Higgins CM, Chun J. Non-proliferative effects of lysophosphatidic acid enhance cortical growth and folding. *Nat Neurosci*. 2003;6:1292-1299.
13. Olianas MC, Dedoni S, Onali P. LPA1 is a key mediator of intracellular signalling and neuroprotection triggered by tetracyclic antidepressants in hippocampal neurons. *J Neurochem*. 2017;143:183-197.
14. Contos JJ, Fukushima N, Weiner JA, Kaushal D, Chun J. Requirement for the lpA1 lysophosphatidic acid receptor gene in normal suckling behavior. *Proc Natl Acad Sci U S A*. 2000;97:13384-13389.

15. Spohr TC, Choi JW, Gardell SE, et al. Lysophosphatidic acid receptor-dependent secondary effects via astrocytes promote neuronal differentiation. *J Biol Chem*. 2008;283:7470-7479.
16. Wheeler NA, Lister JA, Fuss B. The Autotaxin-Lysophosphatidic Acid Axis Modulates Histone Acetylation and Gene Expression during Oligodendrocyte Differentiation. *J Neurosci*. 2015;35: 11399-11414.
17. Fukushima N, Weiner JA, Kaushal D, et al. Lysophosphatidic acid influences the morphology and motility of young, postmitotic cortical neurons. *Mol Cell Neurosci*. 2002;20:271-282.
18. Weiner JA, Hecht JH, Chun J. Lysophosphatidic acid receptor gene vzg-1/lpA1/edg-2 is expressed by mature oligodendrocytes during myelination in the postnatal murine brain. *J Comp Neurol*. 1998;398:587-598.
19. Allard J, Barron S, Trottier S, et al. Edg-2 in myelin-forming cells: isoforms, genomic mapping, and exclusion in Charcot-Marie-Tooth disease. *Glia*. 1999;26:176-185.
20. Cervera P, Tirard M, Barron S, et al. Immunohistological localization of the myelinating cell-specific receptor LP(A1). *Glia*. 2002;38:126-136.
21. Yu N, Lariosa-Willingham KD, Lin FF, Webb M, Rao TS. Characterization of lysophosphatidic acid and sphingosine-1-phosphate-mediated signal transduction in rat cortical oligodendrocytes. *Glia*. 2004;45:17-27.
22. Hecht JH, Weiner JA, Post SR, Chun J. Ventricular zone gene-1 (vzg-1) encodes a lysophosphatidic acid receptor expressed in neurogenic regions of the developing cerebral cortex. *J Cell Biol*. 1996;135:1071-1083.
23. An S, Goetzl EJ, Lee H. Signaling mechanisms and molecular characteristics of G protein-coupled receptors for lysophosphatidic acid and sphingosine 1-phosphate. *J Cell Biochem*. 1998;72(suppl 30–31):147-157.
24. Bandoh K, Aoki J, Hosono H, et al. Molecular cloning and characterization of a novel human G-protein-coupled receptor, EDG7, for lysophosphatidic acid. *J Biol Chem*. 1999;274:27776-27785.
25. Noguchi K, Ishii S, Shimizu T. Identification of p2y9/GPR23 as a novel G protein-coupled receptor for lysophosphatidic acid, structurally distant from the Edg family. *J Biol Chem*. 2003;278: 25600-25606.
26. Lee CW, Rivera R, Gardell S, Dubin AE, Chun J. GPR92 as a new G12/13- and Gq-coupled lysophosphatidic acid receptor that increases cAMP, LPA5. *J Biol Chem*. 2006;281:23589-23597.
27. Yanagida K, Masago K, Nakanishi H, et al. Identification and characterization of a novel lysophosphatidic acid receptor, p2y5/LPA6. *J Biol Chem*. 2009;284:17731-17741.
28. Choi JW, Herr DR, Noguchi K, et al. LPA receptors: subtypes and biological actions. *Annu Rev Pharmacol Toxicol*. 2010;50: 157-186.
29. Kihara Y, Maceyka M, Spiegel S, Chun J. Lysophospholipid receptor nomenclature review: IUPHAR Review 8. *Br J Pharmacol*. 2014;171:3575-3594.
30. Moolenaar WH, Kranenburg O, Postma FR, Zondag GC. Lysophosphatidic acid: G-protein signalling and cellular responses. *Curr Opin Cell Biol*. 1997;9:168-173.
31. Ishii I, Contos JJ, Fukushima N, Chun J. Functional comparisons of the lysophosphatidic acid receptors, LP(A1)/VZG-1/EDG-2, LP(A2)/EDG-4, and LP(A3)/EDG-7 in neuronal cell lines using a retrovirus expression system. *Mol Pharmacol*. 2000;58:895-902.
32. Lee D, Suh DS, Lee SC, Tigyi GJ, Kim JH. Role of autotaxin in cancer stem cells. *Cancer Metastasis Rev*. 2018;37(2-3):509-518.
33. Yanagida K, Ishii S, Hamano F, Noguchi K, Shimizu T. LPA4/p2y9/GPR23 mediates rho-dependent morphological changes in a rat neuronal cell line. *J Biol Chem*. 2007;282:5814-5824.
34. Savaskan NE, Rocha L, Kotter MR, et al. Autotaxin (NPP-2) in the brain: cell type-specific expression and regulation during development and after neurotrauma. *Cell Mol Life Sci*. 2007;64: 230-243.
35. Pasvogel AE, Miketova P, Moore IM. Cerebrospinal fluid phospholipid changes following traumatic brain injury. *Biol Res Nurs*. 2008;10:113-120.
36. Crack PJ, Zhang M, Morganti-Kossmann MC, et al. Anti-lysophosphatidic acid antibodies improve traumatic brain injury outcomes. *J Neuroinflammation*. 2014;11:37.
37. Harrison SM, Reavill C, Brown G, et al. LPA1 receptor-deficient mice have phenotypic changes observed in psychiatric disease. *Mol Cell Neurosci*. 2003;24:1170-1179.
38. Mirendil H, Thomas EA, De Loera C, Okada K, Inomata Y, Chun J. LPA signaling initiates schizophrenia-like brain and behavioral changes in a mouse model of prenatal brain hemorrhage. *Transl Psychiatry*. 2015;5:e541.
39. Mills GB, Moolenaar WH. The emerging role of lysophosphatidic acid in cancer. *Nat Rev Cancer*. 2003;3:582-591.
40. Kishi Y, Okudaira S, Tanaka M, et al. Autotaxin is overexpressed in glioblastoma multiforme and contributes to cell motility of glioblastoma by converting lysophosphatidylcholine to lysophosphatidic acid. *J Biol Chem*. 2006;281:17492-17500.
41. Ueda H, Matsunaga H, Olaposi OI, Nagai J. Lysophosphatidic acid: Chemical signature of neuropathic pain. *Biochim Biophys Acta*. 1831;2013:61-73.
42. Ueda H. Lysophosphatidic acid signaling is the definitive mechanism underlying neuropathic pain. *Pain*. 2017;158(suppl 1): S55-S65.
43. Ohuchi H, Hamada A, Matsuda H, et al. Expression patterns of the lysophospholipid receptor genes during mouse early development. *Dev Dyn*. 2008;237:3280-3294.
44. Khandoga AL, Fujiwara Y, Goyal P, et al. Lysophosphatidic acid-induced platelet shape change revealed through LPA(1-5) receptor-selective probes and albumin. *Platelets*. 2008;19: 415-427.
45. El Waly B, Macchi M, Cayre M, Durbec P. Oligodendrogenesis in the normal and pathological central nervous system. *Front Neurosci*. 2014;8:145.
46. Farhy-Tselnicker I, Allen NJ. Astrocytes, neurons, synapses: a tripartite view on cortical circuit development. *Neural Dev*. 2018;13:7.
47. Ye X, Fukushima N, Kingsbury MA, Chun J. Lysophosphatidic acid in neural signaling. *Neuroreport*. 2002;13:2169-2175.
48. Saper CB. An open letter to our readers on the use of antibodies. *J Comp Neurol*. 2005;493:477-478.
49. Couchman JR. Commercial antibodies: the good, bad, and really ugly. *J Histochem Cytochem*. 2009;57:7-8.
50. Noguchi K, Herr D, Mutoh T, Chun J. Lysophosphatidic acid (LPA) and its receptors. *Curr Opin Pharmacol*. 2009;9:15-23.
51. Spohr TC, Dezonne RS, Rehen SK, Gomes FC. LPA-primed astrocytes induce axonal outgrowth of cortical progenitors by activating PKA signaling pathways and modulating extracellular matrix proteins. *Front Cell Neurosci*. 2014;8:296.

52. Furukawa A, Kita K, Toyomoto M, et al. Production of nerve growth factor enhanced in cultured mouse astrocytes by glycerophospholipids, sphingolipids, and their related compounds. *Mol Cell Biochem*. 2007;305:27-34.
53. Möller T, Contos JJ, Musante DB, Chun J, Ransom BR. Expression and function of lysophosphatidic acid receptors in cultured rodent microglial cells. *J Biol Chem*. 2001;276:25946-25952.
54. Tham CS, Lin FF, Rao TS, Yu N, Webb M. Microglial activation state and lysophospholipid acid receptor expression. *Int J Dev Neurosci*. 2003;21:431-443.
55. An S, Bleu T, Hallmark OG, Goetzl EJ. Characterization of a novel subtype of human G protein-coupled receptor for lysophosphatidic acid. *J Biol Chem*. 1998;273:7906-7910.
56. McGiffert C, Contos JJ, Friedman B, Chun J. Embryonic brain expression analysis of lysophospholipid receptor genes suggests roles for s1p(1) in neurogenesis and s1p(1-3) in angiogenesis. *FEBS Lett*. 2002;531:103-108.
57. Walker TL, Overall RW, Vogler S, et al. Lysophosphatidic Acid Receptor Is a Functional Marker of Adult Hippocampal Precursor Cells. *Stem Cell Reports*. 2016;6:552-565.
58. Im DS, Heise CE, Harding MA, et al. Molecular cloning and characterization of a lysophosphatidic acid receptor, Edg-7, expressed in prostate. *Mol Pharmacol*. 2000;57:753-759.
59. Contos JJ, Ishii I, Chun J. Lysophosphatidic acid receptors. *Mol Pharmacol*. 2000;58:1188-1196.
60. Contos JJ, Chun J. The mouse lp(A3)/Edg7 lysophosphatidic acid receptor gene: genomic structure, chromosomal localization, and expression pattern. *Gene*. 2001;267:243-253.
61. Lee CW, Rivera R, Dubin AE, Chun J. LPA(4)/GPR23 is a lysophosphatidic acid (LPA) receptor utilizing G(s)-, G(q)/G(i)-mediated calcium signaling and G(12/13)-mediated Rho activation. *J Biol Chem*. 2007;282:4310-4317.
62. Lee Z, Cheng CT, Zhang H, et al. Role of LPA4/p2y9/GPR23 in negative regulation of cell motility. *Mol Biol Cell*. 2008;19:5435-5445.
63. Chun J, Hla T, Lynch KR, Spiegel S, Moolenaar WH. International Union of Basic and Clinical Pharmacology. LXXVIII. Lysophospholipid receptor nomenclature. *Pharmacol Rev*. 2010;62:579-587.
64. Geach TJ, Faas L, Devader C, et al. An essential role for LPA signalling in telencephalon development. *Development*. 2014;141:940-949.
65. Plastira I, Bernhart E, Goeritzer M, et al. 1-Oleyl-lysophosphatidic acid (LPA) promotes polarization of BV-2 and primary murine microglia towards an M1-like phenotype. *J Neuroinflammation*. 2016;13:205.
66. Mitra N, Sinha S, Ramya TNC, Surolia A. N-linked oligosaccharides as outfitters for glycoprotein folding, form and function. *Trends Biochem Sci*. 2006;31:156-163.
67. Marino K, Bones J, Kattla JJ, Rudd PM. A systematic approach to protein glycosylation analysis: a path through the maze. *Nat Chem Biol*. 2010;6:713-723.
68. Kohno T, Igarashi Y. Roles for N-glycosylation in the dynamics of Edg-1/S1P1 in sphingosine 1-phosphate-stimulated cells. *Glycoconj J*. 2004;21:497-501.
69. Jalink K, Eichholtz T, Postma FR, van Corven EJ, Moolenaar WH. Lysophosphatidic acid induces neuronal shape changes via a novel, receptor-mediated signaling pathway: similarity to thrombin action. *Cell Growth Differ*. 1993;4:247-255.
70. Jalink K, Hordijk PL, Moolenaar WH. Growth factor-like effects of lysophosphatidic acid, a novel lipid mediator. *Biochim Biophys Acta*. 1994;1198:185-196.
71. Tigyi G, Fischer DJ, Sebok A, Marshall F, Dyer DL, Miledi R. Lysophosphatidic acid-induced neurite retraction in PC12 cells: neurite-protective effects of cyclic AMP signaling. *J Neurochem*. 1996;66:549-558.
72. Kozma R, Sarner S, Ahmed S, Lim L. Rho family GTPases and neuronal growth cone remodelling: relationship between increased complexity induced by Cdc42Hs, Rac1, and acetylcholine and collapse induced by RhoA and lysophosphatidic acid. *Mol Cell Biol*. 1997;17:1201-1211.
73. Kranenburg O, Poland M, Gebbink M, Oomen L, Moolenaar WH. Dissociation of LPA-induced cytoskeletal contraction from stress fiber formation by differential localization of RhoA. *J Cell Sci*. 1997;110(pt 19):2417-2427.
74. Kranenburg O, Poland M, van Horck FP, Drechsel D, Hall A, Moolenaar WH. Activation of RhoA by lysophosphatidic acid and Galpha12/13 subunits in neuronal cells: induction of neurite retraction. *Mol Biol Cell*. 1999;10:1851-1857.
75. Fukushima N, Kimura Y, Chun J. A single receptor encoded by vzg-1/lpA1/edg-2 couples to G proteins and mediates multiple cellular responses to lysophosphatidic acid. *Proc Natl Acad Sci U S A*. 1998;95:6151-6156.
76. Sayas CL, Moreno-Flores MT, Avila J, Wandosell F. The neurite retraction induced by lysophosphatidic acid increases Alzheimer's disease-like Tau phosphorylation. *J Biol Chem*. 1999;274:37046-37052.
77. Ishii I, Fukushima N, Ye X, Chun J. Lysophospholipid receptors: signaling and biology. *Annu Rev Biochem*. 2004;73:321-354.
78. Kim SN, Park JG, Lee EB, Kim SS, Yoo YS. Characterization of epidermal growth factor receptor function in lysophosphatidic acid signaling in PC12 cells. *J Cell Biochem*. 2000;76:386-393.
79. Arimura N, Kaibuchi K. Neuronal polarity: from extracellular signals to intracellular mechanisms. *Nat Rev Neurosci*. 2007;8:194-205.
80. Lloyd B, Tao Q, Lang S, Wylie C. Lysophosphatidic acid signaling controls cortical actin assembly and cytoarchitecture in Xenopus embryos. *Development*. 2005;132:805-816.
81. Lowery LA, Vactor DV. The trip of the tip: understanding the growth cone machinery. *Nat Rev Mol Cell Biol*. 2009;10:332-343.
82. Nürnberg A, Bräuer AU, Wettschureck N, Offermanns S. Antagonistic Regulation of Neurite Morphology through Gq/G11 and G12/G13. *J Biol Chem*. 2008;283:35526-35531.
83. Ishikawa R, Kohama K. Actin-binding proteins in nerve cell growth cones. *J Pharmacol Sci*. 2007;105:6-11.
84. Tojima T, Akiyama H, Itofusa R, et al. Attractive axon guidance involves asymmetric membrane transport and exocytosis in the growth cone. *Nat Neurosci*. 2007;10:58-66.
85. Lai YJ, Chen CS, Lin WC, Lin FT. c-Src-mediated phosphorylation of TRIP6 regulates its function in lysophosphatidic acid-induced cell migration. *Mol Cell Biol*. 2005;25:5859-5868.
86. Lai YJ, Lin WC, Lin FT. PTPL1/FAP-1 negatively regulates TRIP6 function in lysophosphatidic acid-induced cell migration. *J Biol Chem*. 2007;282:24381-24387.
87. Trimbuch T, Beed P, Vogt J, et al. Synaptic PRG-1 modulates excitatory transmission via lipid phosphate-mediated signaling. *Cell*. 2009;138:1222-1235.

88. Fukushima N, Chun J. The LPA receptors. *Prostaglandins*. 2001; 64:21-32.
89. Tabata K, Baba K, Shiraishi A, Ito M, Fujita N. The orphan GPCR GPR87 was deorphanized and shown to be a lysophosphatidic acid receptor. *Biochem Biophys Res Commun*. 2007;363:861-866.
90. Murakami M, Shiraishi A, Tabata K, Fujita N. Identification of the orphan GPCR, P2Y(10) receptor as the sphingosine-1-phosphate and lysophosphatidic acid receptor. *Biochem Biophys Res Commun*. 2008;371:707-712.
91. Pasternack SM, von Kugelgen I, Aboud KA, et al. G protein-coupled receptor P2Y5 and its ligand LPA are involved in maintenance of human hair growth. *Nat Genet*. 2008;40:329-334.
92. Oka S, Ota R, Shima M, Yamashita A, Sugiura T. GPR35 is a novel lysophosphatidic acid receptor. *Biochem Biophys Res Commun*. 2010;395:232-237.
93. Yanagida K, Kurikawa Y, Shimizu T, Ishii S. Current progress in non-Edg family LPA receptor research. *Biochim Biophys Acta*. 1831;2013:33-41.
94. Contos JJ, Ishii I, Fukushima N, et al. Characterization of lpa (2) (Edg4) and lpa(1)/lpa(2) (Edg2/Edg4) lysophosphatidic acid receptor knockout mice: signaling deficits without obvious phenotypic abnormality attributable to lpa(2). *Mol Cell Biol*. 2002; 22:6921-6929.
95. Brewer GJ, Torricelli JR, Evege EK, Price PJ. Optimized survival of hippocampal neurons in B27-supplemented Neurobasal, a new serum-free medium combination. *J Neurosci Res*. 1993;35:567-576.
96. Chen Y, Balasubramaniyan V, Peng J, et al. Isolation and culture of rat and mouse oligodendrocyte precursor cells. *Nat Protoc*. 2007;2:1044-1051.
97. Watkins TA, Emery B, Mulinyawe S, Barres BA. Distinct stages of myelination regulated by gamma-secretase and astrocytes in a rapidly myelinating CNS coculture system. *Neuron*. 2008;60: 555-569.
98. Temple S, Raff MC. Differentiation of a bipotential glial progenitor cell in a single cell microculture. *Nature*. 1985;313:223-225.
99. Witte H, Neukirchen D, Bradke F. Microtubule stabilization specifies initial neuronal polarization. *J Cell Biol*. 2008;180:619-632.
100. Livak KJ, Schmittgen TD. Analysis of relative gene expression data using real-time quantitative PCR and the 2(-Delta Delta C (T)) Method. *Methods*. 2001;25:402-408.
101. Tobin AB, Wheatley M. G-protein-coupled receptor phosphorylation and palmitoylation. *Methods Mol Biol*. 2004;259:275-281.

How to cite this article: Suckau O, Gross I, Schrötter S, et al. LPA_1, LPA_2, LPA_4, and LPA_6 receptor expression during mouse brain development. *Developmental Dynamics*. 2019;248:375–395. https://doi.org/10.1002/dvdy.23